

Lepton masses and mixings, and muon anomalous magnetic moment in an extended $B - L$ model with type I seesaw mechanism

V. V. Vien^{*,†}, Hoang Ngoc Long^{2,‡} and A. E. Cárcamo Hernández^{3,§}

¹*Institute of Applied Technology, Thu Dau Mot University, Binh Duong Province, Vietnam,
Department of Physics, Tay Nguyen University, DakLak province, Vietnam.*

²*Institute of Physics, Vietnam Academy of Science and Technology, 10 Dao Tan, Ba Dinh, 10000 Hanoi, Vietnam.*

³*Department of Physics, Universidad Técnica Federico Santa María,
Casilla 110-V, Valparaíso, Chile,*

Centro Científico-Tecnológico de Valparaíso, Casilla 110-V, Valparaíso, Chile,

Millennium Institute for Subatomic physics at high energy frontier - SAPHIR, Fernandez Concha 700, Santiago, Chile.

(Dated: August 24, 2022)

We propose a $B - L$ model combined with the $S_4 \times Z_3 \times Z_4$ discrete symmetry which successfully explains the recent $3 + 1$ sterile - active neutrino data. The smallness of neutrino mass is obtained through the type-I seesaw mechanism. The active-active and sterile-active neutrino mixing angles are predicted to be consistent with the recent constraints in which $0.3401(0.3402) \leq \sin^2 \theta_{12} \leq 0.3415(0.3416)$, $0.456(0.433) \leq \sin^2 \theta_{23} \leq 0.544(0.545)$, $2.00(2.018) \leq 10^2 \times \sin^2 \theta_{13} \leq 2.405(2.424)$, $156(140.8) \leq \delta_{CP}^{(o)} \leq 172(167.2)$ for normal (inverted) ordering of the three neutrino scenario, and $0.015(0.022) \leq s_{14}^2 \leq 0.045(0.029)$, $0.005(0.0095) \leq s_{24}^2 \leq 0.012(0.012)$, $0.003(0.009) \leq s_{34}^2 \leq 0.011$ for normal (inverted) ordering of the $3 + 1$ neutrino scenario. Our model predicts flavour conserving leptonic neutral scalar interactions and successfully explains the muon $g - 2$ anomaly.

I. INTRODUCTION

Recently, there have been experimental observations that cannot be explained by the three-neutrino oscillation framework [1–13]. However, these observations could be explained by adding at least one additional neutrino (called sterile neutrino) with mass in the eV range having non-trivial mixing with active neutrinos. The mentioned sterile neutrinos are singlets under $SU(2)_L$ which do not take part in the weak interaction but mix with the active ones that can be verified in the oscillation experiments. Nowadays, there are a number of schemes favouring the existence of sterile neutrinos, including the (3+1) scheme [13–29] in which one sterile neutrino with mass in eV scale is heavier than the three active ones; The (3+1+1) scheme [30–34] in which one sterile neutrino with mass in eV scale and the other is much heavier than 1 eV; The (1+3+1) scheme [35–37] in which one of the sterile neutrinos is lighter than the three active ones and the other is heavier; The (3+2) scheme [38–44] in which the two sterile neutrinos are lighter than the three active ones are added to the standard three-neutrino oscillation framework. Among the schemes with sterile neutrinos, the one with one additional sterile neutrino with mass in the eV range (called four neutrino scheme) is the simplest extension of standard three neutrino mixing that can accommodate the anomalous results of short-baseline neutrino oscillations. Among four neutrino schemes, the 3+1 scheme is preferred because the 1+3 scheme whose one sterile neutrino is lighter than the active ones and the three active neutrinos are in eV scale is ruled out by Cosmology while the 2+2 scheme is not suitable with the atmospheric and the solar neutrino oscillation data. Currently, the neutrino mass squared differences and the mixing angles in the three-neutrino scheme[45] and 3+1 neutrino mixing angles[46], at the best-fit points and 3σ range, are shown in Table I. Besides, the 3σ CL ranges on the magnitude of the elements of the leptonic mixing matrix, for three neutrino scheme, are [47]:

$$|U_{\text{with SK-atm}}^{3\sigma}| = \begin{pmatrix} 0.801 \rightarrow 0.845 & 0.513 \rightarrow 0.579 & 0.143 \rightarrow 0.155 \\ 0.234 \rightarrow 0.500 & 0.417 \rightarrow 0.689 & 0.637 \rightarrow 0.776 \\ 0.271 \rightarrow 0.535 & 0.477 \rightarrow 0.694 & 0.613 \rightarrow 0.756 \end{pmatrix}. \quad (1)$$

One notable attribute of discrete symmetries is that they provide an explanation of the neutrino oscillation data. For the $3 + 1$ scheme, the $U(1)_{B-L}$ extension with S_3 symmetry was presented in Ref. [48] without mentioning

* Corresponding author

†Electronic address: vovanvien@tdmu.edu.vn

‡Electronic address: hmlong@iop.vast.vn

§Electronic address: antonio.carcamo@usm.cl

Table I: The neutrino oscillation data for three-neutrino scheme at 3σ range and the best fit points taken from [45], and 3+1 neutrino mixing constraints taken from Ref. [46]

Parameters	3σ range (best fit)	
	Normal hierarchy (NH)	Inverted hierarchy (IH)
$\Delta m_{21}^2 (10^{-5} \text{ eV}^2)$	$6.94 \rightarrow 8.14 (7.50)$	$6.94 \rightarrow 8.14 (7.50)$
$ \Delta m_{31}^2 (10^{-3} \text{ eV}^2)$	$2.47 \rightarrow 2.63 (2.55)$	$2.37 \rightarrow 2.53 (2.45)$
$s_{12}^2/10^{-1}$	$2.71 \rightarrow 3.69 (3.18)$	$2.71 \rightarrow 3.69 (3.18)$
$s_{23}^2/10^{-1}$	$4.34 \rightarrow 6.10 (5.74)$	$4.33 \rightarrow 6.08 (5.78)$
$s_{13}^2/10^{-2}$	$2.000 \rightarrow 2.405 (2.200)$	$2.018 \rightarrow 2.424 (2.225)$
δ/π	$0.71 \rightarrow 1.99 (1.08)$	$1.11 \rightarrow 1.96 (1.58)$
s_{14}^2	$0.0098 \rightarrow 0.0310$	$0.0098 \rightarrow 0.0310$
s_{24}^2	$0.0059 \rightarrow 0.0262$	$0.0059 \rightarrow 0.0262$
s_{34}^2	$0 \rightarrow 0.0369$	$0 \rightarrow 0.0369$

the sterile-active neutrino mass and mixing which has been addressed in Ref. [49] with the results achieved at the first-order approximation, and only the normal mass spectrum was mentioned. The sterile neutrino issue has also been considered in Refs. [50–57] with the A_4 symmetry and a very large amount of scalar fields, which is substantially different than the model considered in this paper whose scalar sector has a moderate amount of particle content. Namely, in Refs. [50, 51] the Standard Model (SM) symmetry is enlarged by the inclusion of the $A_4 \times Z_3 \times U(1)_R$ discrete group. In Ref. [52], the SM symmetry is enlarged by the $A_4 \times Z_4$ symmetry in which only $|U_{e4}|$ has been predicted without $|U_{\mu 4}|$ and $|U_{\tau 4}|$; in Ref. [53], the SM symmetry is enlarged by the symmetry $A_4 \times Z_3 \times Z'_3 \times U(1)_R$ where two doublets and seventeen singlets are used; in Ref. [54], the symmetry $A_4 \times Z_3 \times Z_4$ is added to the SM in which up to three Higgs doublets and twelve singlets are considered in the scalar sector; in Ref. [55] the symmetry $A_4 \times Z_4$ is added to the SM in which one doublets and up to twelve singlet scalars are introduced; in Ref. [56], the symmetry $A_4 \times C_4 \times C_6 \times C_2 \times U(1)_s$ is added to the SM in which one doublets and up to twelve singlets are used, and only the normal mass spectrum is satisfied, and in Ref. [57], the symmetry $A_4 \times Z_3 \times Z_4$ is added to the $B - L$ in which one Higgs doublet and up to eleven singlets are considered in the scalar sector and without mention in the muon anomalous magnetic moment. Thus, it would be useful to build a S_4 flavoured model with a much more economical scalar content. To our knowledge, A_4 has not been considered before in the 3+1 scheme with $B - L$ extension.

This paper is organized as follows. The description of the model is presented in section II. Its implications in lepton masses and mixings as well as the corresponding numerical analysis is presented in section III. Section IV is devoted to the muon anomalous magnetic moment. Finally, some conclusions are given in section V. Appendix B provides the scalar potential of the model.

II. THE MODEL

The $B - L$ gauge model [58, 59] is supplemented by one discrete symmetry S_4 along with two Abelian symmetries Z_3 and Z_4 . Further, three right-handed neutrinos ν_R , one sterile neutrino ν_s , one $SU(2)_L$ doublet (H') and four singlet scalars ($\phi, \varphi, \rho, \phi_s$) are additional introduction to the $B - L$ model. Three right-handed neutrinos and three left-handed leptons ψ_L are grouped in **3** under S_4 symmetry whereas the first right-handed charged leptons l_{1R} is assigned as **1** and the two others are grouped in **2** under the S_4 symmetry. The sterile neutrino ν_s is assigned as **1** under the S_4 symmetry. The particle content of the model under consideration¹ and its corresponding assignments under the symmetry $SU(2)_L \times U(1)_Y \times U(1)_{B-L} \times S_4 \times Z_3 \times Z_4 \equiv \Gamma$ are shown in Table II.

¹ Under $SU(3)_C$ symmetry, all leptons and scalars are singlets.

Table II: The particle and scalar contents of the model.

Fields	ψ_L	$l_{1R}(l_{\alpha R})$	$H(H')$	$\phi(\varphi)$	ρ	χ	ϕ_s	ν_R	ν_s
$[\text{SU}(2)_L, \text{U}(1)_Y]$	[2, -1/2]	[1, -1]	[2, 1/2]	[1, 0]	[1, 0]	[1, 0]	[1, 0]	[1, 0]	[1, 0]
$\text{U}(1)_{B-L}$	-1	-1	0	0	0	2	0	-1	-1
S_4	3	1(2)	1(1')	3	1	1	3	3	1
Z_3	ω	1	1	$\omega(1)$	1	ω	ω^2	ω	ω^2
Z_4	i	1	1	i	i	1	i	1	$-i$

With the above specified particle content, the following five dimensional Yukawa interactions invariant under the symmetries of the model arise:

$$\begin{aligned} -\mathcal{L}_{clep} = & \frac{x_1}{\Lambda} (\bar{\psi}_L l_{1R})_3 (H\phi)_3 + \frac{x_2}{\Lambda} (\bar{\psi}_L l_{\alpha R})_3 (H\phi)_3 + \frac{x_3}{\Lambda} (\bar{\psi}_L l_{\alpha R})_{3'} (H'\phi)_{3'} \\ & + \frac{x_{1\nu}}{\Lambda} (\bar{\psi}_L \nu_R)_1 (\tilde{H}\rho)_1 + \frac{x_{2\nu}}{\Lambda} (\bar{\psi}_L \nu_R)_3 (\tilde{H}\varphi)_3 + \frac{x_{3\nu}}{\Lambda} (\bar{\psi}_L \nu_R)_{3'} (\tilde{H}'\varphi)_{3'} \\ & + \frac{y_\nu}{2} (\bar{\nu}_R^c \nu_R)_1 \chi + \frac{y_s}{\Lambda} (\bar{\nu}_s^c \nu_R)_3 (\chi \phi_s)_3 + H.c. \end{aligned} \quad (2)$$

In Eq. (2), Λ is the cut-off scale of the theory, y_ν, y_s, x_k and $x_{k\nu}$ ($k = 1, 2, 3$) are dimensionless constants. The VEVs of scalar fields satisfying the scalar potential minimum condition, presented in section B, are given as follows

$$\begin{aligned} \langle H \rangle = (0 & v)^T, \quad \langle H' \rangle = (0 & v')^T, \quad \langle \phi \rangle = (\langle \phi_1 \rangle, \langle \phi_2 \rangle, \langle \phi_3 \rangle), \quad \langle \phi_1 \rangle = \langle \phi_2 \rangle = \langle \phi_3 \rangle = v_\phi, \\ \langle \varphi \rangle = (0 & \langle \varphi_2 \rangle 0), \quad \langle \varphi_2 \rangle = v_\varphi, \quad \langle \rho \rangle = v_\rho, \quad \langle \chi \rangle = v_\chi, \quad \langle \phi_s \rangle = (\langle \phi_{1s} \rangle 0 \langle \phi_{3s} \rangle), \quad \langle \phi_{1s} \rangle = \langle \phi_{3s} \rangle = v_s. \end{aligned} \quad (3)$$

In fact the electroweak symmetry breaking scale is one order of magnitude lower than TeV scale and the $B - L$ scale is assumed to be at the TeV scale, i.e.,

$$v' \sim v = 1.23 \times 10^2 \text{ GeV}, \quad v_\chi = 10^3 \text{ GeV}. \quad (4)$$

Furthermore, in order to have very heavy right handed Majorana neutrino masses, thus allowing the implementation of the type I seesaw mechanism that produces the tiny masses of the active neutrinos, the VEVs of flavons ϕ, φ, ρ and ϕ_s are assumed to be at a very high scale:

$$v_\phi \sim v_\varphi \sim v_\rho \sim v_{\phi_s} = 10^{11} \text{ GeV}. \quad (5)$$

It is interesting to note that each of additional symmetry $U(1)_{B-L}, S_4, Z_3$ and Z_4 plays a crucial role in forbidding the unwanted terms, which are listed in Table V of Appendix A, to obtain the lepton mass matrices in Eqs. (7) and (19). Furthermore, there exist invariant terms via Weinberg operators whose dimensions greater than or equal to six, $\frac{1}{\Lambda^{2(k+l+1)}} (\bar{\psi}_L \psi_L^c) (\tilde{H}^2 \chi^*) (\mathbf{H}^\dagger \mathbf{H})^k (\mathbf{P}^* \mathbf{P})^l$ with $k, l = 0, 1, 2, \dots$; $\mathbf{H} = H, H'$, and $\mathbf{P} = \phi, \varphi, \rho, \chi, \phi_s$. The fact that $v_H \ll v_P \ll \Lambda$. Hence, the neutrino mass obtained by those Weinberg operators, $v_H \left(\frac{v_H}{\Lambda}\right)^{2k+1} \left(\frac{v_P}{\Lambda}\right)^{2l+1}$, is very small compared to the one obtained by the type-I seesaw mechanism as in Eq.(19) and thus have been ignored.

III. NEUTRINO MASS AND MIXING

A. Lepton mass and mixing in the three neutrino framework

From the Yukawa interactions in Eq. (2), and using the tensor product rules of the S_4 discrete group [60], together with the VEVs of scalar fields in Eq. (3), the charged lepton mass Lagrangian is written in the form:

$$\mathcal{L}_{cl}^{\text{mass}} = -(\bar{l}_{1L} \bar{l}_{2L} \bar{l}_{3L}) M_l (l_{1R} l_{2R} l_{3R})^T + H.c, \quad (6)$$

where

$$M_l = \begin{pmatrix} x_1 v \frac{v_\phi}{\Lambda} & \frac{v_\phi}{\Lambda} (x_2 v + x_3 v') & \frac{v_\phi}{\Lambda} (x_2 v - x_3 v') \\ x_1 v \frac{v_\varphi}{\Lambda} & \omega^2 \frac{v_\varphi}{\Lambda} (x_2 v + x_3 v') & \omega \frac{v_\varphi}{\Lambda} (x_2 v - x_3 v') \\ x_1 v \frac{v_\rho}{\Lambda} & \omega \frac{v_\rho}{\Lambda} (x_2 v + x_3 v') & \omega^2 \frac{v_\rho}{\Lambda} (x_2 v - x_3 v') \end{pmatrix}, \quad (7)$$

which is diagonalized as, $U_l^\dagger M_l U_r = \text{diag}(m_e, m_\mu, m_\tau)$, with

$$U_l^\dagger = \frac{1}{\sqrt{3}} \begin{pmatrix} 1 & 1 & 1 \\ 1 & \omega & \omega^2 \\ 1 & \omega^2 & \omega \end{pmatrix}, \quad U_r = \mathbf{I}_{3 \times 3} \quad (\omega = e^{\frac{i2\pi}{3}}), \quad (8)$$

$$m_e = \sqrt{3}x_1 v \frac{v_\phi}{\Lambda}, \quad m_{\mu,\tau} = \sqrt{3} \frac{v_\phi}{\Lambda} (x_2 v \pm x_3 v'). \quad (9)$$

Equation (8) tells us that U_l is non trivial and hence it will affect on the lepton mixing matrix. Furthermore, Eq. (9) shows that m_μ and m_τ are distinguished by v' . This is the reason why H' is additionally introduced to H .

Furthermore, assuming the gauge singlet scalar fields adjure VEVs much larger than the electroweak symmetry breaking scale, the scalar spectrum at low energies is the same as in the 2HDM theory. Then, the physical CP even and CP odd neutral scalar fields are given by:

$$H_R^0 = \sin \alpha h - \cos \alpha H, \quad H_R'^0 = -\cos \alpha h - \sin \alpha H, \quad (10)$$

$$H_I^0 = \cos \beta G_Z + \sin \beta A^0, \quad H_I'^0 = \sin \beta G_Z - \cos \beta A^0, \quad (11)$$

where G_Z is the Goldstone boson associated with the longitudinal component of the gauge boson Z , h is the 126 GeV SM like Higgs, H is the heavy CP even Higgs, A is the heavy CP odd Higgs boson, $\tan \beta = \frac{v}{v'}$ and α is the mixing angle in the neutral scalar sector. Then, the leptonic Yukawa interactions involving neutral scalar fields are given by:

$$\begin{aligned} \mathcal{L}_Y^h &= \sqrt{\frac{3}{2}} y_1 \sin \alpha \bar{e}_L h e_R + \sqrt{\frac{3}{2}} (y_2 \sin \alpha - y_3 \cos \alpha) \bar{\mu}_L h \mu_R \\ &\quad + \sqrt{\frac{3}{2}} (y_2 \sin \alpha + y_3 \cos \alpha) \bar{\tau}_L h \tau_R + h.c, \end{aligned} \quad (12)$$

$$\begin{aligned} \mathcal{L}_Y^{H^0} &= -\sqrt{\frac{3}{2}} y_1 \cos \alpha \bar{e}_L H^0 e_R + \sqrt{\frac{3}{2}} (y_2 \cos \alpha + y_3 \sin \alpha) \bar{\mu}_L H^0 \mu_R \\ &\quad + \sqrt{\frac{3}{2}} (y_2 \cos \alpha - y_3 \sin \alpha) \bar{\tau}_L H^0 \tau_R + h.c, \end{aligned} \quad (13)$$

$$\begin{aligned} \mathcal{L}_Y^{A^0} &= i\sqrt{\frac{3}{2}} y_1 \sin \beta \bar{e}_L A^0 e_R + i\sqrt{\frac{3}{2}} (y_2 \sin \beta - y_3 \cos \beta) \bar{\mu}_L A^0 \mu_R \\ &\quad + i\sqrt{\frac{3}{2}} (y_2 \sin \beta + y_3 \cos \beta) \bar{\tau}_L A^0 \tau_R + h.c, \end{aligned} \quad (14)$$

where

$$y_k = x_k \frac{v_\phi}{\Lambda} \quad (k = 1, 2, 3). \quad (15)$$

Equations (12), (13) and (14) imply that the flavour changing leptonic neutral scalar interactions are absent in our model. Consequently, there are no scalar contributions to the charged lepton flavor violating decays $\tau \rightarrow \mu\gamma$, $\tau \rightarrow e\gamma$ and $\mu \rightarrow e\gamma$. The charged lepton flavor violating decays $\tau \rightarrow \mu\gamma$, $\tau \rightarrow e\gamma$ and $\mu \rightarrow e\gamma$ will receive one loop level contributions due to the electrically charged scalars and right handed Majorana neutrinos, however these contributions will scale with the inverse of fourth power of the model cutoff as well as with the fourth power of the very small neutrino Yukawa coupling, thus making their branching ratios very tiny. Another contributions to the charged lepton flavor violating decays will arise from the virtual exchange of a W gauge boson and sterile neutrinos however those contributions will have very tiny branching ratios as in the SM.

As we will see in the following, our model can successfully accommodate the SM charged lepton masses. Now, comparing the obtained result in Eq. (9) with the experimental values of $m_{e,\mu,\tau}$ [61], $m_e = 0.51099 \text{ MeV}$, $m_\mu = 105.65837 \text{ MeV}$, $m_\tau = 1776.86 \text{ MeV}$, and considering the benchmark point $v = v' = 123 \text{ GeV}$, $v_\phi = 10^{11} \text{ GeV}$ and $\Lambda = 10^{13} \text{ GeV}$, we get:

$$|x_1| \sim 10^{-4}, \quad |x_2| \sim |x_3| \sim 10^{-1}. \quad (16)$$

Furthermore, from the above given leptonic Yukawa interactions and using the benchmark point given above, it follows that the coupling of the 126 GeV SM like Higgs boson with the SM lepton-antilepton pair is about 0.7 the SM expectation.

From the particle content given in Tab. II, we get the following neutrino Yukawa interactions:

$$\begin{aligned} -\mathcal{L}_Y^l &= \frac{x_{1\nu}}{\Lambda} (\bar{\psi}_{1L}\nu_{1R} + \bar{\psi}_{2L}\nu_{2R} + \bar{\psi}_{3L}\nu_{3R}) \tilde{H}\rho \\ &+ \frac{x_{2\nu}}{\Lambda} \left[(\bar{\psi}_{2L}\nu_{3R} + \bar{\psi}_{3L}\nu_{2R})(\tilde{H}\varphi_1) + (\bar{\psi}_{3L}\nu_{1R} + \bar{\psi}_{1L}\nu_{3R})(\tilde{H}\varphi_2) + (\bar{\psi}_{1L}\nu_{2R} + \bar{\psi}_{2L}\nu_{1R})(\tilde{H}\varphi_3) \right] \\ &+ \frac{x_{3\nu}}{\Lambda} \left[(\bar{\psi}_{2L}\nu_{3R} - \bar{\psi}_{3L}\nu_{2R})(\tilde{H}'\varphi_1) + (\bar{\psi}_{3L}\nu_{1R} - \bar{\psi}_{1L}\nu_{3R})(\tilde{H}'\varphi_2) + (\bar{\psi}_{1L}\nu_{2R} - \bar{\psi}_{2L}\nu_{1R})(\tilde{H}'\varphi_3) \right] \\ &+ \frac{y_\nu}{2} (\bar{\nu}_{1R}^c\nu_{1R} + \bar{\nu}_{2R}^c\nu_{2R} + \bar{\nu}_{3R}^c\nu_{3R})\chi + \frac{y_s}{\Lambda} (\bar{\nu}_s^c\nu_{1R}\chi\phi_{1s} + \bar{\nu}_s^c\nu_{2R}\chi\phi_{2s} + \bar{\nu}_s^c\nu_{3R}\chi\phi_{3s}) + \text{H.c.} \end{aligned} \quad (17)$$

With the VEV configuration given in Eq. (3), after symmetry breaking, the 7×7 neutrino mass matrix in the (ν_L^c, ν_R, ν_s) basis takes the form

$$M_\nu^{7 \times 7} = \begin{pmatrix} 0 & M_D & 0 \\ M_D^T & M_R & M_S^T \\ 0 & M_S & 0 \end{pmatrix}, \quad (18)$$

where M_D , M_R and M_S are the Dirac, Majorana and sterile neutrino mass matrices, respectively. They are given by:

$$\begin{aligned} M_D &= \begin{pmatrix} \frac{v_\rho}{\Lambda} vx_{1\nu} & 0 & \frac{v_\varphi}{\Lambda} (vx_{2\nu} - v'x_{3\nu}) \\ 0 & \frac{v_\rho}{\Lambda} vx_{1\nu} & 0 \\ \frac{v_\varphi}{\Lambda} (vx_{2\nu} + v'x_{3\nu}) & 0 & \frac{v_\rho}{\Lambda} vx_{1\nu} \end{pmatrix}, \\ M_R &= y_\nu v_\chi \mathbf{I}, \quad M_S = y_s v_\chi \frac{v_s}{\Lambda} (1 \quad 0 \quad 1). \end{aligned} \quad (19)$$

In the case of $M_D < M_S \ll M_R$, the effective 4×4 light neutrino mass matrix is determined by [50, 52, 54, 56]:

$$M_\nu = - \begin{pmatrix} M_D M_R^{-1} M_D^T & M_D M_R^{-1} M_S^T \\ M_S (M_R^{-1})^T M_D^T & M_S M_R^{-1} M_S^T \end{pmatrix}. \quad (20)$$

The expression (19) shows that, in the neutrino sector, there are five complex parameters, thus implying the existence of ten real parameters. Considering the case of real VEVs for the scalars H, H', ϕ, χ and η while taking the VEV of φ to be complex ($v_\varphi = v_0 e^{i\alpha}$), the phase redefinition of ψ_L and ν_R allows to rotate away the phases of three Yukawa couplings $x_{1\nu}$, y_ν and y_s , reducing to seven parameters. Furthermore, two parameters are absorbed during the formation of the neutrino mass matrix. Thus, there are left five real and dimensionless parameters $k_{2,3}, m, m_s$ and α , where $k_{2,3}, m$ and m_s are defined as follows

$$k_2 = \frac{v_0}{v_\rho} \frac{x_{2\nu}}{x_{1\nu}}, \quad k_3 = \frac{v_0}{v_\rho} \frac{v'}{v} \frac{x_{3\nu}}{x_{1\nu}}, \quad m = \frac{v^2 v_\rho^2 x_{1\nu}^2}{\Lambda^2 v_\chi y_\nu}, \quad m_s = \frac{2 v_\chi v_s^2 y_s^2}{\Lambda^2 y_\nu}. \quad (21)$$

Combining Eqs.(19) and (20) yields the 4×4 active-sterile mass matrix in the explicit form

$$M_\nu^{4 \times 4} = - \begin{pmatrix} m \begin{pmatrix} 1 + (k_2 - k_3)^2 e^{2i\alpha} & 0 & 2k_2 e^{i\alpha} \\ 0 & 1 & 0 \\ 2k_2 e^{i\alpha} & 0 & 1 + (k_2 + k_3)^2 e^{2i\alpha} \end{pmatrix} \sqrt{\frac{mm_s}{2}} \begin{pmatrix} 1 + (k_2 - k_3)e^{i\alpha} \\ 0 \\ 1 + (k_2 + k_3)e^{i\alpha} \end{pmatrix} \\ \sqrt{\frac{mm_s}{2}} \begin{pmatrix} 1 + (k_2 - k_3)e^{i\alpha} & 0 & 1 + (k_2 + k_3)e^{i\alpha} \end{pmatrix} \end{pmatrix}. \quad (22)$$

In the case of $M_D < M_S$, one can apply the type-I seesaw mechanism on Eq.(20) to get the active neutrino mass matrix as [50, 52, 54, 56]

$$\begin{aligned} M_\nu &= M_D M_R^{-1} M_S^T (M_S M_R^{-1} M_S^T)^{-1} M_S M_R^{-1} M_D^T - M_D M_R^{-1} M_D^T \\ &= \frac{m}{2} \begin{pmatrix} -[(k_2 - k_3)e^{i\alpha} - 1]^2 & 0 & 1 + (k_2^2 - k_3^2)e^{2i\alpha} - 2e^{i\alpha}k_2 \\ 0 & -2 & 0 \\ 1 + (k_2^2 - k_3^2)e^{2i\alpha} - 2e^{i\alpha}k_2 & 0 & -[(k_2 + k_3)e^{i\alpha} - 1]^2 \end{pmatrix}. \end{aligned} \quad (23)$$

We note that M_ν is complex because $m, k_{2,3}$ and α are real parameters. Hence, to determine the active neutrino masses, we define a Hermitian matrix \mathbf{m}_ν^2 given by

$$\mathbf{m}_\nu^2 = M_\nu M_\nu^\dagger = \frac{m^2 k_0}{2} \begin{pmatrix} k_- & 0 & 2k_3^2 - k_0 - i2k_3 \sin \alpha \\ 0 & \frac{2}{k_0} & 0 \\ 2k_3^2 - k_0 + i2k_3 \sin \alpha & 0 & k_+ \end{pmatrix}, \quad (24)$$

where

$$k_0 = 1 + k_2^2 + k_3^2 - 2k_2 \cos \alpha, \quad k_{\mp} = 1 + (k_2 \mp k_3)^2 - 2(k_2 \mp k_3) \cos \alpha. \quad (25)$$

The squared matrix \mathbf{m}_{ν}^2 in Eq. (24) is diagonalized by the rotation matrix U_{ν} satisfying

$$U_{\nu}^{\dagger} \mathbf{m}_{\nu}^2 U_{\nu} = \begin{cases} \begin{pmatrix} 0 & 0 & 0 \\ 0 & m^2 & 0 \\ 0 & 0 & m^2 k_0^2 \end{pmatrix}, & U_{\nu} = \begin{pmatrix} g_0(g_1 + ig_2) & 0 & -r_0(g_1 + ig_2) \\ 0 & 1 & 0 \\ \frac{1}{\sqrt{2}g_0} & 0 & \frac{1}{\sqrt{2}r_0} \end{pmatrix} \text{ for NH,} \\ \begin{pmatrix} m^2 k_0^2 & 0 & 0 \\ 0 & m^2 & 0 \\ 0 & 0 & 0 \end{pmatrix}, & U_{\nu} = \begin{pmatrix} -r_0(g_1 + ig_2) & 0 & g_0(g_1 + ig_2) \\ 0 & 1 & 0 \\ \frac{1}{\sqrt{2}r_0} & 0 & \frac{1}{\sqrt{2}g_0} \end{pmatrix} \text{ for IH,} \end{cases} \quad (26)$$

where

$$g_0 = \sqrt{\frac{k_0}{k_-}}, \quad r_0 = \sqrt{\frac{k_0}{k_+}}, \quad g_1 = \frac{1}{\sqrt{2}} - \frac{\sqrt{2}k_3^2}{k_0}, \quad g_2 = \frac{\sqrt{2}k_3 \sin \alpha}{k_0}. \quad (27)$$

The corresponding leptonic mixing matrix is

$$U_{\text{lep}} = U_L^{\dagger} U_{\nu} = \begin{cases} \frac{1}{\sqrt{3}} \begin{pmatrix} \frac{1}{\sqrt{2}g_0} + g_0(g_1 + ig_2) & 1 & \frac{1}{\sqrt{2}r_0} - (g_1 + ig_2)r_0 \\ \frac{\omega^2}{\sqrt{2}g_0} + g_0(g_1 + ig_2) & \omega & \frac{\omega^2}{\sqrt{2}r_0} - (g_1 + ig_2)r_0 \\ \frac{\omega}{\sqrt{2}g_0} + g_0(g_1 + ig_2) & \omega^2 & \frac{\omega}{\sqrt{2}r_0} - (g_1 + ig_2)r_0 \end{pmatrix} & \text{for NH,} \\ \frac{1}{\sqrt{3}} \begin{pmatrix} \frac{1}{\sqrt{2}r_0} - (g_1 + ig_2)r_0 & 1 & \frac{1}{\sqrt{2}g_0} + g_0(g_1 + ig_2) \\ \frac{\omega^2}{\sqrt{2}r_0} - (g_1 + ig_2)r_0 & \omega & \frac{\omega^2}{\sqrt{2}g_0} + g_0(g_1 + ig_2) \\ \frac{\omega}{\sqrt{2}r_0} - (g_1 + ig_2)r_0 & \omega^2 & \frac{\omega}{\sqrt{2}g_0} + g_0(g_1 + ig_2) \end{pmatrix} & \text{for IH.} \end{cases} \quad (28)$$

Three light neutrino masses are given by

$$\begin{cases} m_1^2 = 0, & m_2^2 = m^2, & m_3^2 = k_0^2 m^2 \quad \text{for NH,} \\ m_1^2 = k_0^2 m^2, & m_2^2 = m^2, & m_3^2 = 0 \quad \text{for IH,} \end{cases} \quad (29)$$

which implies the neutrino mass ordering should be either $(0, m, m k_0)$ or $(m k_0, m, 0)$. It is important to note that in the considered model both NH ($m_1 < m_2 < m_3$) and IH ($m_3 < m_1 < m_2$) are satisfied due to the fact that k_0 in Eq. (25) can be greater or less than the one in the case of k_2 and k_3 are real parameters. Hence, the model can predict both NH and IH spectrum which are consistent with the recent experimental data [45] and different from that of Ref. [56] in which only the NH is allowed.

In the three-neutrino scheme [61], the lepton mixing angles are determined from Eq. (28),

$$s_{13}^2 = |U_{e3}|^2 = \begin{cases} \frac{2}{3} \frac{k_3^2}{k_0} & \text{for NH,} \\ \frac{2}{3} - \frac{2}{3} \frac{k_3^2}{k_0} & \text{for IH,} \end{cases} \quad (30)$$

$$s_{12}^2 = \frac{|U_{e2}|^2}{1 - |U_{e3}|^2} = \frac{1}{3c_{13}^2} \quad \text{for both NH and IH,} \quad (31)$$

$$s_{23}^2 = \frac{|U_{\mu 3}|^2}{1 - |U_{e3}|^2} = \begin{cases} \frac{1}{2} + \frac{\sqrt{3}k_3 \sin \alpha}{3k_0 - 2k_3^2} & \text{for NH,} \\ \frac{1}{2} - \frac{\sqrt{3}k_3 \sin \alpha}{k_0 + 2k_3^2} & \text{for IH,} \end{cases} \quad (32)$$

where $s_{ij} = \sin \theta_{ij}$, $c_{ij} = \cos \theta_{ij}$, $t_{12} = \frac{s_{12}}{c_{12}}$ and $t_{23} = \frac{s_{23}}{c_{23}}$ with θ_{ij} are neutrino mixing angles.

Furthermore, from Eqs. (29), we can express m and k_0 in terms of two observables Δm_{21}^2 and Δm_{31}^2 as follows:

$$m = \begin{cases} \sqrt{\Delta m_{21}^2} & \text{for NH,} \\ \sqrt{\Delta m_{21}^2 - \Delta m_{31}^2} & \text{for IH,} \end{cases} \quad (33)$$

$$k_0 = \begin{cases} \frac{\sqrt{\Delta m_{31}^2}}{m} & \text{for NH,} \\ \frac{\sqrt{-\Delta m_{31}^2}}{m} & \text{for IH.} \end{cases} \quad (34)$$

The fact that the neutrino mass ordering can be normal ($m_1 < m_2 < m_3$) or inverted ($m_3 < m_1 < m_2$) depending on the sign of Δm_{31}^2 [45, 62]. We will show that the considered model can provide the satisfied explanation on neutrino masses and mixings data, for both three-neutrino scheme and 3 + 1 scheme, given in Table I.

B. 3+1 sterile-active neutrino mixing

In the case of $M_D < M_S$, the mass of the 4th mass eigenstate is given by[50, 52, 54, 56],

$$m_4 = M_S M_R^{-1} M_S^T = m_s. \quad (35)$$

Combining Eqs. (29) and (35) yields:

$$m_s = m_4 = \begin{cases} \sqrt{\Delta m_{41}^2} & \text{for NH,} \\ \sqrt{m^2 k_0^2 + \Delta m_{41}^2} & \text{for IH.} \end{cases} \quad (36)$$

The 4×4 neutrino mixing matrix is given by [50, 52, 54, 56]:

$$U = U_L^\dagger U_\nu = \begin{pmatrix} U_L^\dagger (1 - \frac{1}{2} R R^\dagger) U_\nu & U_L^\dagger R \\ -R^\dagger U_\nu & 1 - \frac{1}{2} R^\dagger R \end{pmatrix}, \quad (37)$$

where R is given by [50, 52, 54, 56]

$$R = M_D M_R^{-1} M_S^T (M_S M_R^{-1} M_S^T)^{-1} = \sqrt{\frac{m}{2m_s}} \begin{pmatrix} 1 + (k_2 - k_3)e^{i\alpha} \\ 0 \\ 1 + (k_2 + k_3)e^{i\alpha} \end{pmatrix}. \quad (38)$$

Combining Eqs. (8) and (38), we find that the strength of the active-sterile mixing is given by

$$U_L^\dagger R = \sqrt{\frac{m}{6m_s}} \begin{pmatrix} 2 + 2k_2 e^{i\alpha} \\ [\omega^2(k_2 + k_3) + k_2 - k_3] e^{i\alpha} - \omega \\ [\omega(k_2 + k_3) + k_2 - k_3] e^{i\alpha} - \omega^2 \end{pmatrix} \equiv \begin{pmatrix} U_{e4} \\ U_{\mu 4} \\ U_{\tau 4} \end{pmatrix}, \quad (39)$$

which leads to

$$\begin{aligned} s_{14}^2 &= |U_{e4}|^2 = \frac{2}{3} \frac{m}{m_s} (1 + k_2^2 + 2k_2 \cos \alpha), \\ s_{24}^2 &= \frac{|U_{\mu 4}|^2}{1 - |U_{e4}|^2} = \frac{1 + k_2^2 + 3k_3^2 + 2k_2 \cos \alpha + 2\sqrt{3}k_3 \sin \alpha}{\frac{6m_s}{m} - 4(1 + k_2^2 + 2k_2 \cos \alpha)}, \\ s_{34}^2 &= \frac{|U_{\tau 4}|^2}{1 - |U_{e4}|^2 - |U_{\mu 4}|^2} = \frac{1 + k_2^2 + 3k_3^2 + 2k_2 \cos \alpha - 2\sqrt{3}k_3 \sin \alpha}{\frac{6m_s}{m} - (5 + 5k_2^2 + 3k_3^2 + 10k_2 \cos \alpha + 2\sqrt{3}k_3 \sin \alpha)}. \end{aligned} \quad (40)$$

C. Effective neutrino mass parameter and Jarlskog invariant

The Jarlskog invariant, obtained from Eq. (28), has the form [61, 63–65]

$$J_{CP} = \text{Im}(U_{12} U_{23} U_{13}^* U_{22}^*) = \begin{cases} \frac{k_3(k_2 - \cos \alpha)}{3\sqrt{3}k_0} & \text{for NH,} \\ -\frac{k_3(k_2 - \cos \alpha)}{3\sqrt{3}k_0} & \text{for IH.} \end{cases} \quad (41)$$

The effective neutrino masses get the following forms [66–68],

$$m_{\beta}^{(3)} = \sqrt{\sum_{i=1}^3 |U_{ei}|^2 m_i^2} = \sqrt{\frac{m^2}{3} + \frac{m^2 k_0 [(2k_3^2 - k_0 + k_+)^2 + 4k_3^2 \sin^2 \alpha]}{6k_+}}, \quad (42)$$

$$\begin{aligned} \langle m_{ee}^{(3)} \rangle &= \left| \sum_{i=1}^3 U_{ei}^2 m_i \right| \\ &= \frac{m}{6} \sqrt{\frac{16k_3^2 \sin^2 \alpha (2k_3^2 - k_0 + k_+)^2 + [(k_+ - k_0 + 2k_3^2)^2 - 4k_3^2 \sin^2 \alpha + 2k_+]^2}{k_+^2}}, \end{aligned} \quad (43)$$

$$\begin{aligned} m_{\beta} &= \sqrt{\sum_{i=1}^4 |U_{ei}|^2 m_i^2} = \left\{ \frac{m^2}{3} + \frac{m^2 k_0 [(2k_3^2 - k_0 + k_+)^2 + 4k_3^2 \sin^2 \alpha]}{6k_+} \right. \\ &\quad \left. + \frac{2mm_s}{3} [(k_2 \cos \alpha + 1)^2 + k_2^2 \sin^2 \alpha] \right\}^{\frac{1}{2}}, \end{aligned} \quad (44)$$

$$\begin{aligned} \langle m_{ee} \rangle &= \left| \sum_{i=1}^4 U_{ei}^2 m_i \right| = \frac{m}{3} \left\{ 16 \sin^2 \alpha [2k_2 k_+ (k_2 \cos \alpha + 1) + k_0 k_3 - 2k_3^3 - k_3 k_+]^2 \right. \\ &\quad + [k_0^2 + 6k_+ + 4k_2 k_+ (k_2 \cos \alpha + 2) \cos \alpha - 2k_0 (2k_3^2 + k_+)] \\ &\quad \left. - 4 (k_2^2 k_+ + k_3^2) \sin^2 \alpha + (2k_3^2 + k_+)^2 \right\}^{\frac{1}{2}}. \end{aligned} \quad (45)$$

D. Numerical analysis

Firstly, provided that s_{13} is located inside the 3σ experimentally allowed range² taken from Ref. [45], i.e., $s_{13}^2 \in (2.000, 2.405)10^{-2}$ for NH and $s_{13}^2 \in (2.018, 2.424)10^{-2}$ for IH, from Eq. (31), we predict solar mixing angle

$$s_{12}^2 \in \begin{cases} (0.3401, 0.3415) & \text{for NH,} \\ (0.3402, 0.3416) & \text{for IH,} \end{cases} \quad (46)$$

which is consistent with the 2σ experimental range given in Ref. [45].

Furthermore, Eqs. (33) and (34) imply that

$$m \in \begin{cases} (8.331, 9.022) \text{ meV for NH,} \\ (49.39, 51.10) \text{ meV for IH,} \end{cases} \quad k_0 \in \begin{cases} (5.51, 6.16) & \text{for NH,} \\ (0.9833, 0.9866) & \text{for IH,} \end{cases} \quad (47)$$

$$\begin{cases} m_1 = 0, \quad m_2 \in (8.331, 9.022) \text{ meV,} \quad m_3 \in (49.70, 51.28) \text{ meV} & \text{for NH,} \\ m_1 \in (48.68, 50.30) \text{ meV,} \quad m_2 \in (49.39, 50.10) \text{ meV,} \quad m_3 = 0 & \text{for IH,} \end{cases} \quad (48)$$

$$\sum_{i=1}^3 m_i \in \begin{cases} (58.03, 60.31) \text{ meV for NH,} \\ (98.07, 101.30) \text{ meV for IH,} \end{cases} \quad (49)$$

provided that the light neutrino mass-squared differences Δm_{21}^2 and Δm_{31}^2 to be varied in 3σ range of Ref. [45] as shown in Table I.

To find the allowed ranges of k_2 , k_3 , m , m_s and α , and predictive ranges of the experimental parameters $\sin^2 \theta_{23}$, $\sin \delta$, $\langle m_{ee} \rangle$ and s_{k4}^2 ($k = 1, 2, 3$), we utilize the observables Δm_{21}^2 , Δm_{31}^2 , Δm_{41}^2 , $\sin^2 \theta_{13}$ and $\sin^2 \theta_{23}$ with values given in Table I³.

² In present work, numbers are displayed with 4 significant digits to the right of the decimal point.

³ As will be mentioned below, at present, there are various experimental bounds on Δm_{41}^2 . In this work, Δm_{41}^2 is assumed in the range of $\Delta m_{41}^2 \in (5.0, 10) \text{ eV}^2$ for NH while $\Delta m_{41}^2 \in (30.0, 50.0) \text{ eV}^2$ for IH.

From Eqs. (25), (30)-(32) and (41), we get:

$$k_2 = \begin{cases} -\frac{1}{s_{13}} \sqrt{\frac{t_N k_\Phi}{2} + \Phi_N + s_{13}^2} & \text{for NH,} \\ \sqrt{1 + \frac{1}{2-3s_{13}^2} \left(\frac{3t_I k_\Phi}{2} + \sqrt{3}\Phi_I \right)} & \text{for IH,} \end{cases} \quad (50)$$

$$k_3 = \begin{cases} \sqrt{\frac{3t_N}{2}} s_{13} & \text{for NH,} \\ \sqrt{\left(1 - \frac{3}{2}s_{13}^2\right) t_I} & \text{for IH,} \end{cases} \quad (51)$$

$$\cos \alpha = \begin{cases} \frac{\sqrt{\frac{t_N k_\Phi}{2} + \Phi_N + s_{13}^2} \left(t_N c_{13}^4 \cos^2 2\theta_{23} + \Phi_N - 2s_{13}^2 \right)}{[t_N(3s_{13}^2 - 2) + 2] s_{13}^3} & \text{for NH,} \\ \frac{\sqrt{2-3s_{13}^2 + \frac{3t_I k_\Phi}{2} + \sqrt{3}\Phi_I} \left(3t_I c_{13}^4 \cos^2 2\theta_{23} + \sqrt{3}\Phi_I + 6s_{13}^2 - 4 \right)}{\sqrt{2-3s_{13}^2} (3t_I s_{13}^2 - 2)} & \text{for IH,} \end{cases} \quad (52)$$

$$\sin \delta_{CP} = \begin{cases} -\frac{\sqrt{t_N k_\Phi + 2(\Phi_N + s_{13}^2)} \left(s_{13} + \frac{t_N c_{13}^4 \cos^2 2\theta_{23} + \Phi_N - 2s_{13}^2}{s_{13}[t_N(3s_{13}^2 - 2) + 2]} \right)}{\sqrt{t_N s_{13}^2} \sin 2\theta_{23} \sqrt{2-3s_{13}^2}} & \text{for NH,} \\ -\frac{s_{13} \sqrt{2-3s_{13}^2 + \frac{3t_I k_\Phi}{2} + \sqrt{3}\Phi_I} \left(\frac{3t_I c_{13}^4 \cos^2 2\theta_{23} + \sqrt{3}\Phi_I + 6s_{13}^2 - 4}{(3s_{13}^2 - 2)(3t_N s_{13}^2 - 2)} + 1 \right)}{\sqrt{6s_{13}^2 s_{23} c_{23}} \sqrt{(2-3s_{13}^2) t_N}} & \text{for IH,} \end{cases} \quad (53)$$

with

$$\Phi_N = \sqrt{(\cos^2 2\theta_{13} - c_{13}^4 \sin^2 2\theta_{23}) (t_N c_{13}^4 \cos^2 2\theta_{23} - 2s_{13}^2) t_N}, \quad (54)$$

$$\Phi_I = \sqrt{(\cos^2 2\theta_{13} - c_{13}^4 \sin^2 2\theta_{23}) (3t_I c_{13}^4 \cos^2 2\theta_{23} + 6s_{13}^2 - 4) t_I}, \quad (55)$$

$$k_\Phi = (6 - 5s_{13}^2)s_{13}^2 + 2(c_{13}^4 \sin^2 2\theta_{23} - 1), \quad (56)$$

$$t_N = \sqrt{\frac{\Delta m_{31}^2}{\Delta m_{21}^2}}, \quad t_I = \sqrt{\frac{-\Delta m_{31}^2}{\Delta m_{21}^2 - \Delta m_{31}^2}}. \quad (57)$$

Equations (50)-(57) imply that k_3 depends on three parameters Δm_{21}^2 , Δm_{31}^2 and s_{13} while k_2 and $\cos \alpha$ depend on four parameters Δm_{21}^2 , Δm_{31}^2 , s_{13} and s_{23} . As a consequence, Eqs. (40)–(57) imply that J_{CP} , $\sin \delta_{CP}$, $\langle m_{ee}^{(3)} \rangle$, $\langle m_{ee} \rangle$ and $m_\beta^{(3)}$ as well as $|U_{ij}|$ ($i = 1, 2, 3$; $j = 1, 3$) depend on four parameters Δm_{21}^2 , Δm_{31}^2 , s_{13} and s_{23} while s_{k4}^2 ($k = 1, 2, 3$) and m_β depend on five parameters Δm_{21}^2 , Δm_{31}^2 , s_{13} , s_{23} and $m_s \equiv m_4 \equiv \sqrt{\Delta m_{41}^2}$ in which three parameters Δm_{21}^2 , Δm_{31}^2 and s_{13} are measured with more accuracy that can be used to constrain the others.

At the best-fit points of Δm_{31}^2 [45], $\Delta m_{31}^2 = 2.55 \times 10^3 \text{ meV}^2$ for NH and $\Delta m_{31}^2 = -2.45 \times 10^3 \text{ meV}^2$ for IH, the parameter k_3 depends on s_{13}^2 and Δm_{21}^2 which is depicted in Fig. 1. This figure implies

$$k_3 \in \begin{cases} (0.41, 0.46) & \text{for NH,} \\ (0.9740, 0.9775) & \text{for IH,} \end{cases} \quad (58)$$

At the best-fit points of two light neutrino mass squared differences taken from Ref. [45], $\Delta m_{31}^2 = 2.55 \times 10^3 \text{ meV}^2$ for NH while $\Delta m_{31}^2 = -2.45 \times 10^3 \text{ meV}^2$ for IH and $\Delta m_{31}^2 = 75.0 \text{ meV}^2$, we get

$$k_0 = \begin{cases} 5.831 & \text{for NH,} \\ 0.985 & \text{for IH,} \end{cases} \quad (59)$$

and the parameters k_2 , $\cos \alpha$, $\sin \delta_{CP}$, $\langle m_{ee}^{(3)} \rangle$, $\langle m_{ee} \rangle$ and $m_\beta^{(3)}$ depend on s_{13} and s_{23} which are, respectively, depicted in Figs. 2, 3, 5, 6, 8 and 9.

Figure 2 implies that

$$k_2 \in \begin{cases} (-3.20, -2.40) & \text{for NH,} \\ (1.13, 1.18) & \text{for IH.} \end{cases} \quad (60)$$

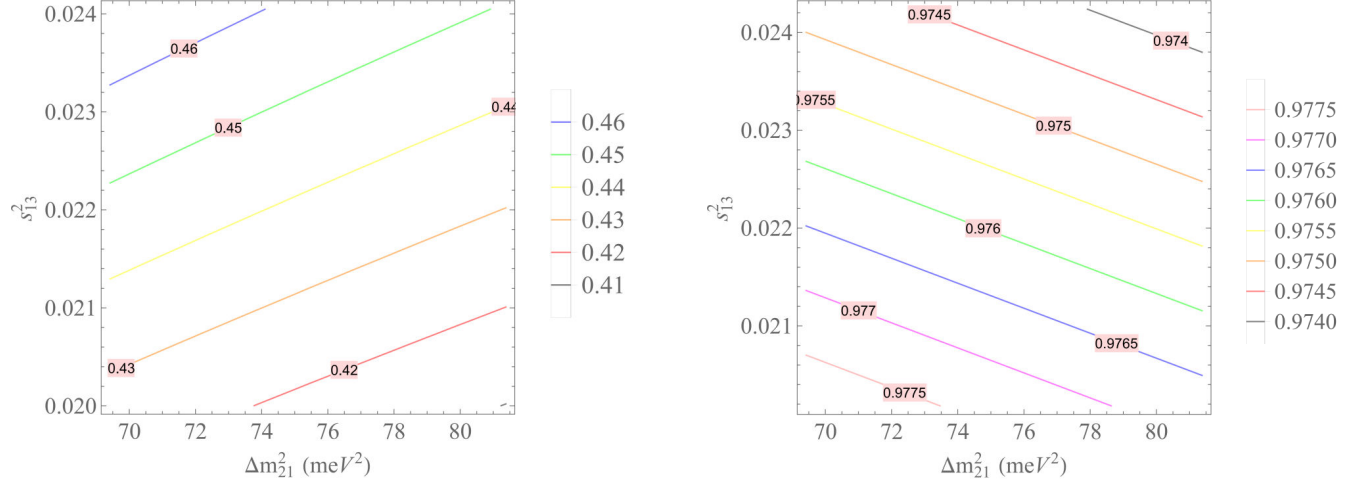


Figure 1: k_3 as a function of s_{13}^2 and Δm_{21}^2 with $\Delta m_{21}^2 \in (69.4, 81.4)$ meV 2 and $s_{13}^2 \in (2.000, 2.405)10^{-2}$ for NH (in the left panel) while $s_{13}^2 \in (2.018, 2.424)10^{-2}$ for IH (in the right panel).

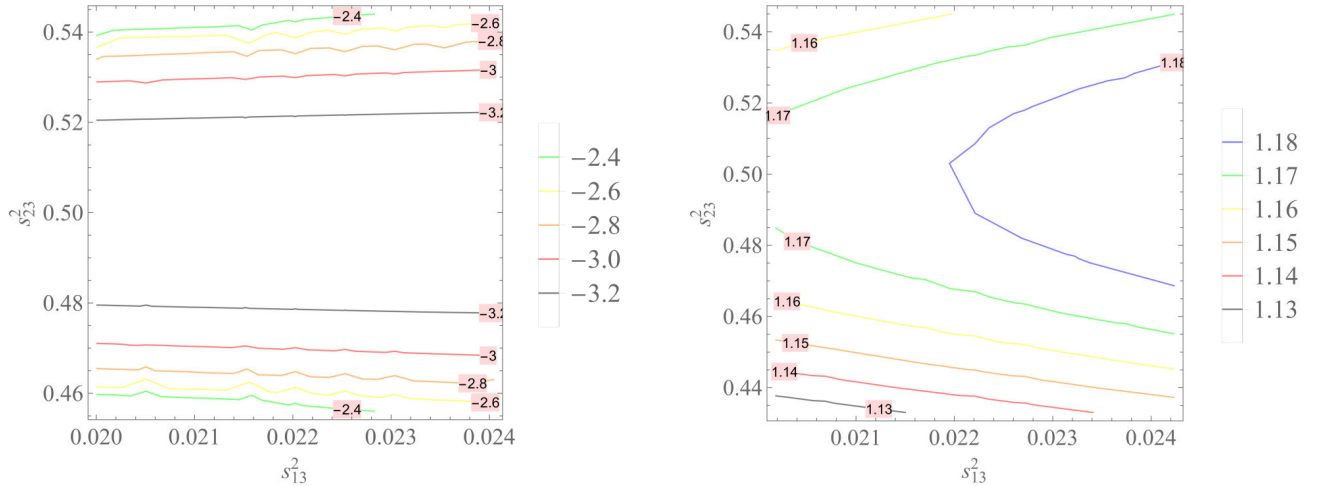


Figure 2: k_2 as a function of s_{23}^2 and s_{13}^2 with $s_{23}^2 \in (0.456, 0.544)$ and $s_{13}^2 \in (2.00, 2.405)10^{-2}$ for NH (in the left panel) while $s_{23}^2 \in (0.433, 0.545)$ and $s_{13}^2 \in (2.018, 2.424)10^{-2}$ for IH (in the right panel).

From figure 3, it follows that:

$$\cos \alpha \in \begin{cases} (-0.90, 0.0) & \text{for NH,} \\ (0.994, 0.999) & \text{for IH,} \end{cases} \quad \text{i.e., } \alpha^{(\circ)} \in \begin{cases} (90.0, 154.0) & \text{for NH,} \\ (2.563, 6.28) & \text{for IH.} \end{cases} \quad (61)$$

The dependence of J_{CP} on s_{23}^2 and s_{13}^2 is depicted in Fig. 4.

Figure 4 implies that the Jarlskog invariant takes the values [61]:

$$J_{CP} \in \begin{cases} (-3.5, -3.0) \times 10^{-2} & \text{for NH,} \\ (-3.4, -2.6) \times 10^{-2} & \text{for IH.} \end{cases} \quad (62)$$

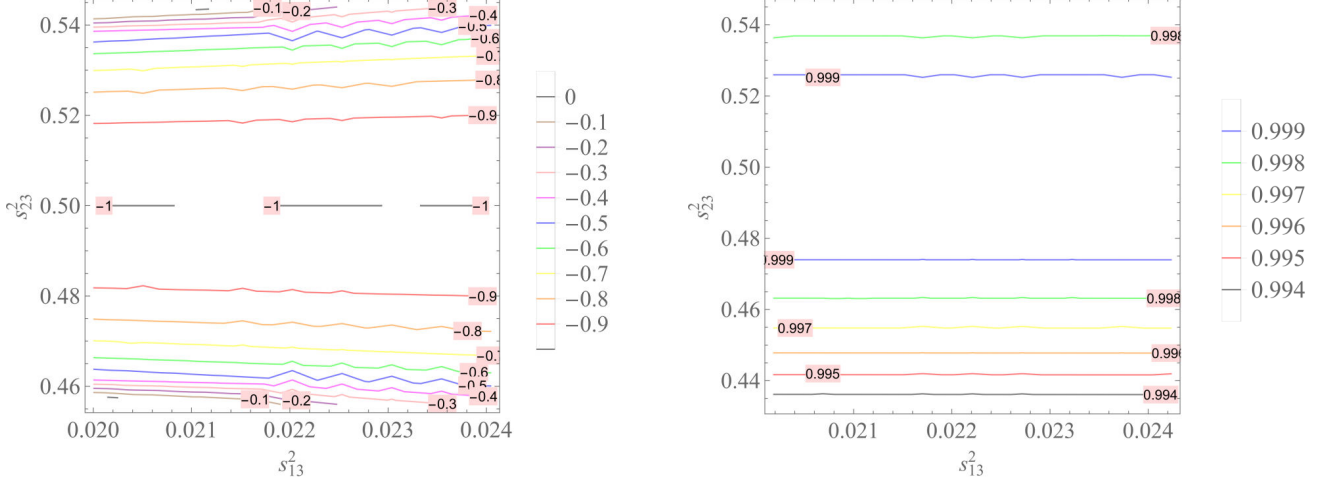


Figure 3: $\cos \alpha$ as a function of s_{23}^2 and s_{13}^2 with $s_{23}^2 \in (0.456, 0.544)$ and $s_{13}^2 \in (2.00, 2.405)10^{-2}$ for NH (in the left panel) while $s_{23}^2 \in (0.433, 0.545)$ and $s_{13}^2 \in (2.018, 2.424)10^{-2}$ for IH (in the right panel).

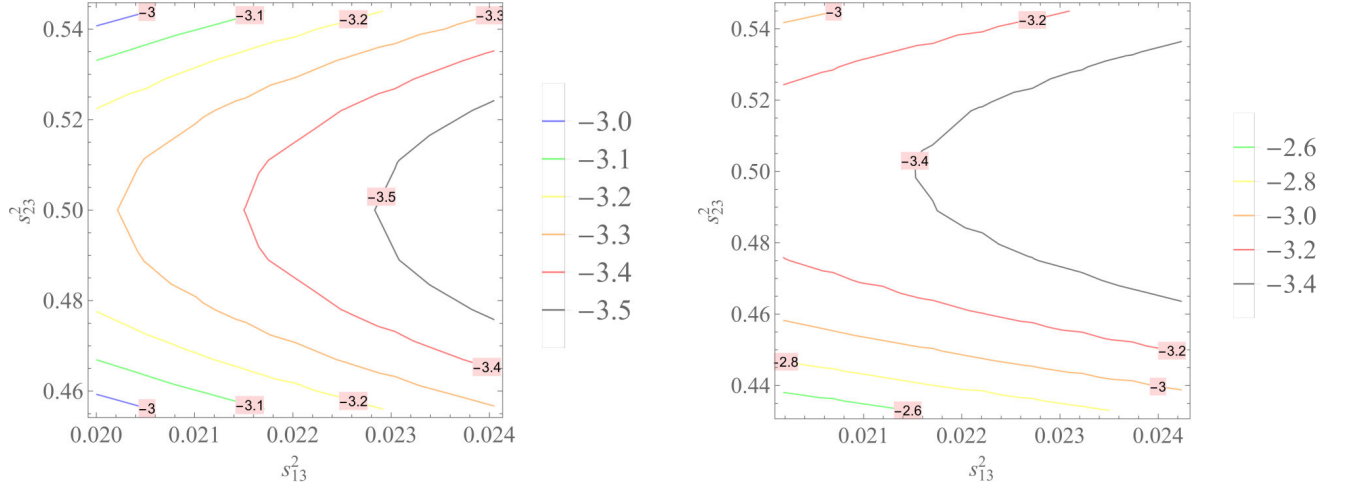


Figure 4: $J_{CP} \times 10^2$ as a function of s_{23}^2 and s_{13}^2 with $s_{23}^2 \in (0.456, 0.544)$ and $s_{13}^2 \in (2.00, 2.405)10^{-2}$ for NH (in the left panel) while $s_{23}^2 \in (0.433, 0.545)$ and $s_{13}^2 \in (2.018, 2.424)10^{-2}$ for IH (in the right panel).

Figure 5 implies that

$$\sin \delta_{CP} \in \begin{cases} (-0.99, -0.91) & \text{for NH,} \\ (-0.975, -0.775) & \text{for IH,} \end{cases} \quad \text{i.e., } \delta_{CP}^{(\circ)} \in \begin{cases} (156.0, 172.0) & \text{for NH,} \\ (140.8, 167.2) & \text{for IH.} \end{cases} \quad (63)$$

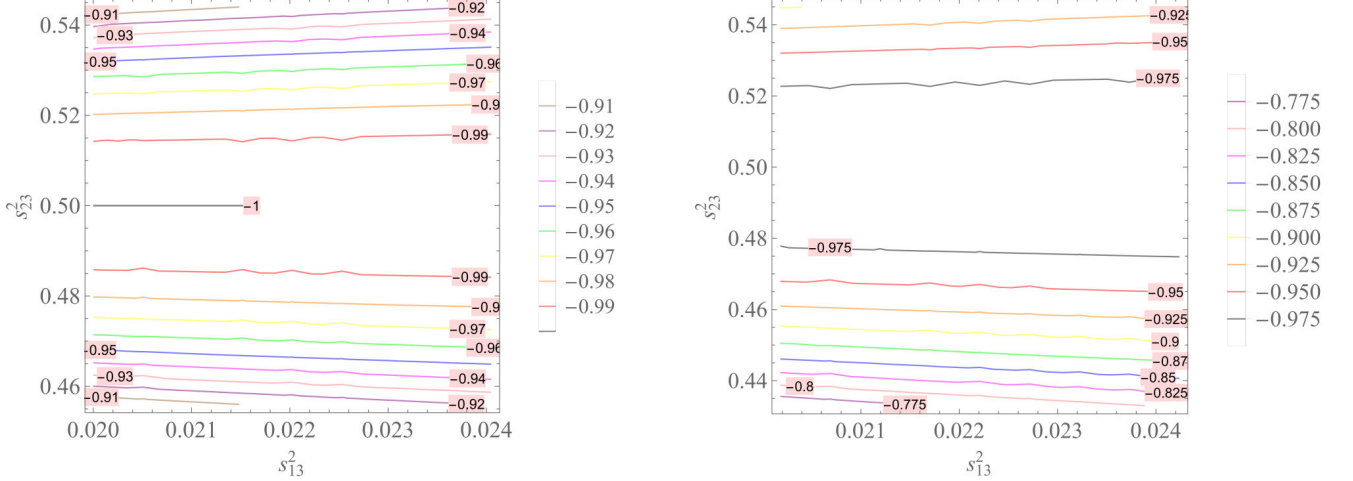


Figure 5: $\sin \delta_{CP}$ as a function of s_{23}^2 and s_{13}^2 with $s_{23}^2 \in (0.456, 0.545)$ and $s_{13}^2 \in (2.00, 2.405)10^{-2}$ for NH (in the left panel) while $s_{23}^2 \in (0.433, 0.545)$ and $s_{13}^2 \in (2.018, 2.424)10^{-2}$ for IH (in the right panel).

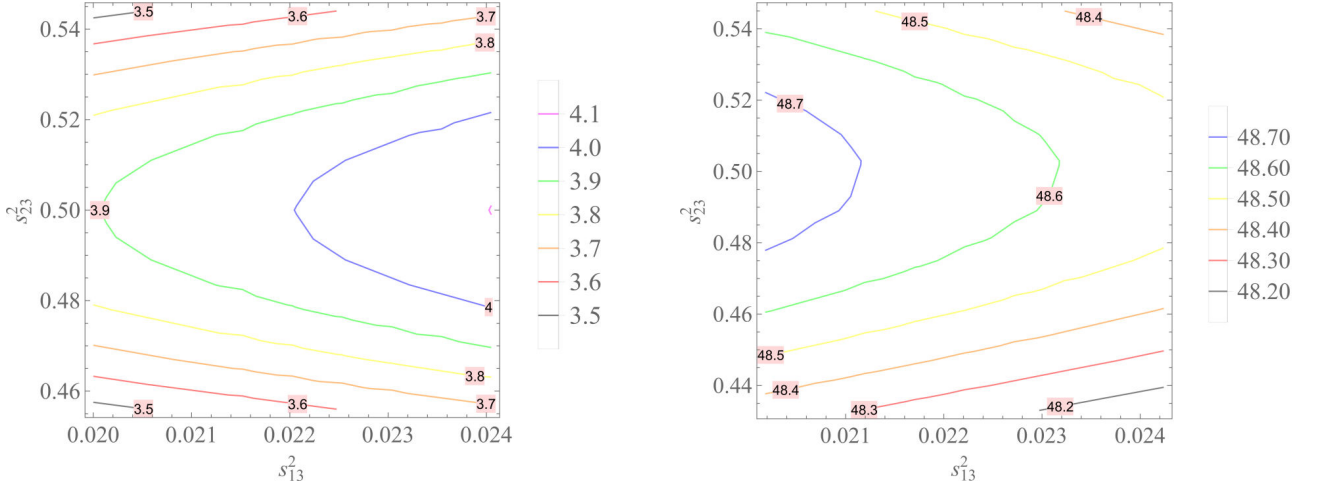


Figure 6: $\langle m_{ee}^{(3)} \rangle$ (meV) as a function of s_{23}^2 and s_{13}^2 with $s_{23}^2 \in (0.456, 0.544)$ and $s_{13}^2 \in (2.00, 2.405)10^{-2}$ for NH (in the left panel) while $s_{23}^2 \in (0.433, 0.545)$ and $s_{13}^2 \in (2.018, 2.424)10^{-2}$ for IH (in the right panel).

Figures 6 and 7 imply that

$$\langle m_{ee}^{(3)} \rangle \in \begin{cases} (3.50, 4.10) \text{ meV} & \text{for NH,} \\ (48.20, 48.70) \text{ meV} & \text{for IH,} \end{cases} \quad (64)$$

$$m_\beta^{(3)} \in \begin{cases} (8.80, 9.20) \text{ meV} & \text{for NH,} \\ (49.16, 49.24) \text{ meV} & \text{for IH,} \end{cases} \quad (65)$$

$$\langle m_{ee} \rangle \in \begin{cases} (40.0, 110.0) \text{ meV} & \text{for NH,} \\ (198.0, 208.0) \text{ meV} & \text{for IH.} \end{cases} \quad (66)$$

We see that the resulting effective neutrino mass for three neutrino scheme in Eqs. (64)-(66), for both NH and IH, are

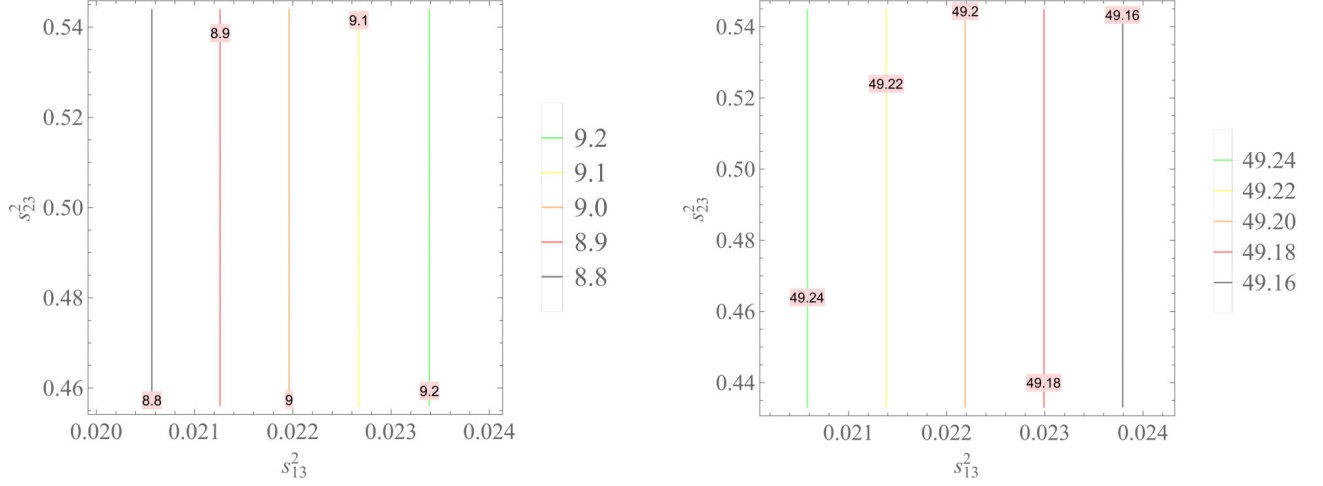


Figure 7: $m_\beta^{(3)}$ (meV) as a function of s_{23}^2 and s_{13}^2 with $s_{23}^2 \in (0.456, 0.544)$ and $s_{13}^2 \in (2.00, 2.405)10^{-2}$ for NH (in the left panel) while $s_{23}^2 \in (0.433, 0.545)$ and $s_{13}^2 \in (2.018, 2.424)10^{-2}$ for IH (in the right panel).

below all the upper limits taken from GERDA [69] $\langle m_{ee} \rangle < (120 \div 260)$ meV, MAJORANA [70] $\langle m_{ee} \rangle < (24 \div 53)$ meV, CUORE [71] $\langle m_{ee} \rangle < (110 \div 500)$ meV, KamLAND-Zen [72] $\langle m_{ee} \rangle < (61 \div 165)$ meV, GERDA [73] $\langle m_{ee} \rangle < (104 \div 228)$ meV, CUORE [74] $\langle m_{ee} \rangle < (75 \div 350)$ meV and CUPID-Mo Collaboration [75] $\langle m_{ee} \rangle < (310 \div 540)$ meV.

The dependence of $\langle m_{ee} \rangle$ on s_{23}^2 and Δm_{41}^2 with $s_{23}^2 \in (0.433, 0.545)$ and $\Delta m_{41}^2 \in (10.0, 30.0)10^6$ meV 2 are depicted in Fig. 8.

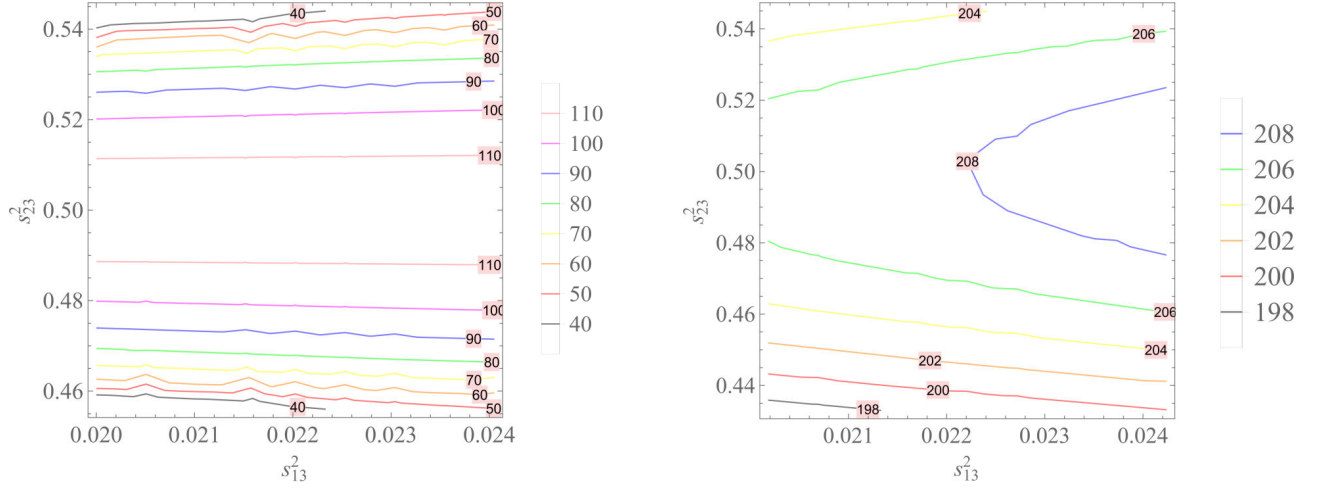


Figure 8: $\langle m_{ee} \rangle$ (meV) as a function of s_{23}^2 and s_{13}^2 with $s_{23}^2 \in (0.456, 0.544)$ and $s_{13}^2 \in (2.00, 2.405)10^{-2}$ for NH (in the left panel) while $s_{23}^2 \in (0.541, 0.598)$ and $s_{13}^2 \in (2.018, 2.424)10^{-2}$ for IH (in the right panel).

The dependences of the absolute values of the entries of the lepton mixing matrix in Eq. (28) on s_{13} and s_{23} are

presented in Figs. 15 and 16 which indicate that

$$|U_{\text{lep}}| \in \begin{cases} \left(\begin{array}{lll} 0.8020 \rightarrow 0.8040 & \frac{1}{\sqrt{3}} & 0.142 \rightarrow 0.154 \\ 0.370 \rightarrow 0.420 & \frac{1}{\sqrt{3}} & 0.700 \rightarrow 0.730 \\ 0.430 \rightarrow 0.470 & \frac{1}{\sqrt{3}} & 0.670 \rightarrow 0.695 \\ 0.8020 \rightarrow 0.8040 & \frac{1}{\sqrt{3}} & 0.144 \rightarrow 0.154 \\ 0.440 \rightarrow 0.490 & \frac{1}{\sqrt{3}} & 0.655 \rightarrow 0.690 \\ 0.340 \rightarrow 0.400 & \frac{1}{\sqrt{3}} & 0.710 \rightarrow 0.745 \end{array} \right) & \text{for NH,} \\ \left(\begin{array}{lll} 0.8020 \rightarrow 0.8040 & \frac{1}{\sqrt{3}} & 0.142 \rightarrow 0.154 \\ 0.370 \rightarrow 0.420 & \frac{1}{\sqrt{3}} & 0.700 \rightarrow 0.730 \\ 0.430 \rightarrow 0.470 & \frac{1}{\sqrt{3}} & 0.670 \rightarrow 0.695 \\ 0.8020 \rightarrow 0.8040 & \frac{1}{\sqrt{3}} & 0.144 \rightarrow 0.154 \\ 0.440 \rightarrow 0.490 & \frac{1}{\sqrt{3}} & 0.655 \rightarrow 0.690 \\ 0.340 \rightarrow 0.400 & \frac{1}{\sqrt{3}} & 0.710 \rightarrow 0.745 \end{array} \right) & \text{for IH.} \end{cases} \quad (67)$$

At the best-fit points of the two light neutrino mass squared differences and reactor neutrino mixing angle taken from Ref. [45], $\Delta m_{31}^2 = 75.0 \text{ meV}^2$ and $\Delta m_{31}^2 = 2.55 \times 10^3 \text{ meV}^2$, $s_{13}^2 = 2.200 \times 10^{-2}$ for NH while $\Delta m_{31}^2 = -2.45 \times 10^3 \text{ meV}^2$, $s_{13}^2 = 2.225 \times 10^{-2}$ for IH, the parameter m_β and s_{k4}^2 ($k = 1, 2, 3$) depend on s_{23} and $m_s = \sqrt{\Delta m_{14}^2}$. At present, there are various experimental bounds on Δm_{41}^2 [6–12, 76–81], for example, $\Delta m_{41}^2 \in (0.01, 1.0) \text{ eV}^2$ [76], $\Delta m_{41}^2 > 10^{-2} \text{ eV}^2$ [8], $\Delta m_{41}^2 = 0.041 \text{ eV}^2$ [78], $\Delta m_{41}^2 \in (0.1, 1.0) \text{ eV}^2$ [77], $\Delta m_{41}^2 \in (0.2, 10.0) \text{ eV}^2$ [9], $\Delta m_{41}^2 \geq 0.1 \text{ eV}^2$ [10], $\Delta m_{41}^2 = 1.0 \text{ eV}^2$ [79, 80], $\Delta m_{41}^2 > 1.5 \text{ eV}^2$ [11], $\Delta m_{41}^2 = 1.7 \text{ eV}^2$ [81], $\Delta m_{41}^2 < 10.0 \text{ eV}^2$ [6] $\Delta m_{41}^2 = 1.45 \text{ eV}^2$ [7]. Thus in this work, Δm_{41}^2 is assumed in the range of $\Delta m_{41}^2 \in (5.0, 10.0) \text{ eV}^2$ for NH while $\Delta m_{41}^2 \in (30.0, 50.0) \text{ eV}^2$ for IH. Going by this assumption, the dependences of m_β and s_{k4}^2 on s_{23} and Δm_{41}^2 , with $s_{23}^2 \in (0.456, 0.544)$ and $\Delta m_{41}^2 \in (5.0, 10.0) \text{ eV}^2$ for NH while $s_{23}^2 \in (0.433, 0.545)$ and $\Delta m_{41}^2 \in (30.0, 50.0) \text{ eV}^2$ for IH, are presented in Figs. 9, 10 and 11, respectively.

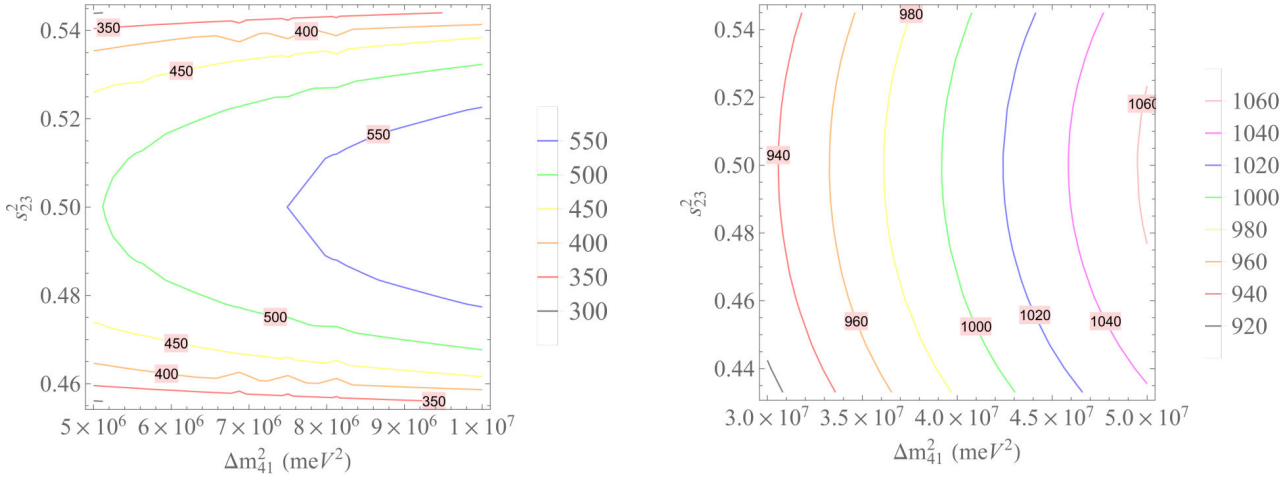


Figure 9: m_β (meV) as a function of s_{23}^2 and s_{13}^2 with $s_{23}^2 \in (0.456, 0.544)$ and $\Delta m_{41}^2 \in (5.0, 10.0) \text{ eV}^2$ for NH (in the left panel) while $s_{23}^2 \in (0.433, 0.545)$ and $\Delta m_{41}^2 \in (30.0, 50.0) \text{ eV}^2$ for IH (in the right panel).

Figures 10–11 show that the considered model predicts the range of s_{14}^2 , s_{24}^2 and s_{34}^2 as follows

$$s_{14}^2 \in \begin{cases} (0.015, 0.045) & \text{for NH,} \\ (0.022, 0.029) & \text{for IH,} \end{cases} \quad (68)$$

$$s_{24}^2 \in \begin{cases} (0.005, 0.012) & \text{for NH,} \\ (0.0095, 0.012) & \text{for IH,} \end{cases} \quad (69)$$

$$s_{34}^2 \in \begin{cases} (0.003, 0.011) & \text{for NH,} \\ (0.009, 0.012) & \text{for IH,} \end{cases} \quad (70)$$

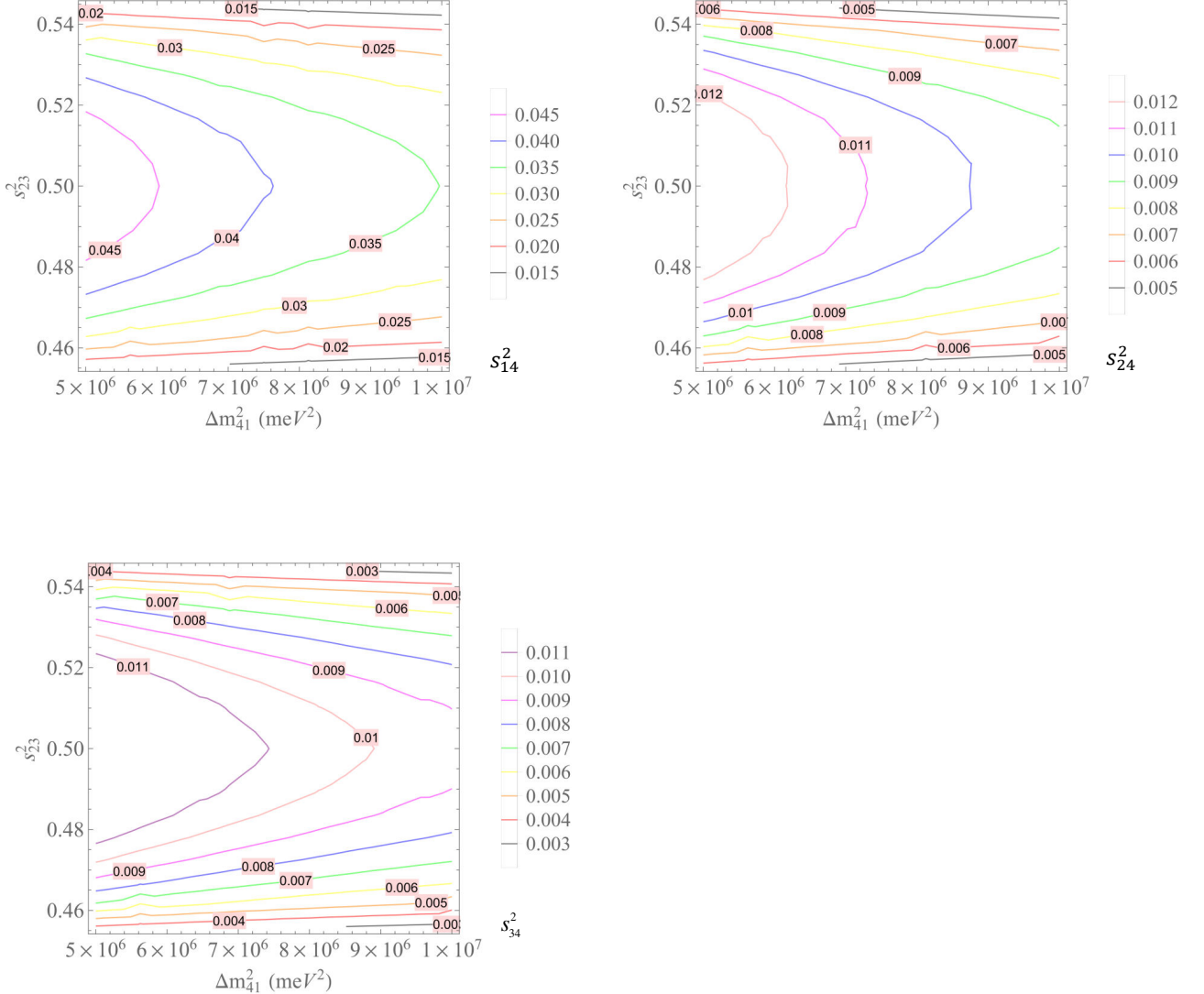


Figure 10: s_{14}^2 , s_{24}^2 and s_{34}^2 as functions of s_{23}^2 and Δm_{41}^2 with $s_{23}^2 \in (0.456, 0.544)$ and $\Delta m_{41}^2 \in (5.0, 10.0)10^6$ meV 2 for NH.

which are in consistent with the constraints given in Tab. I.

Finally, from the above analysis, the obtained parameters of the model are summarized in Table III. In the case $s_{23}^2 = 0.544$ ($\theta_{23} = 47.50^\circ$) and $\Delta m_{41}^2 = 5.0$ eV 2 for NH while $s_{23}^2 = 0.545$ ($\theta_{23} = 47.58^\circ$) and $\Delta m_{41}^2 = 30.0$ eV 2 ($m_s = 4477.23$ meV) for IH, we obtain the parameters as given in Tab. IV and the lepton mixing matrix gets the explicit form:

$$U_{lep} = \begin{cases} \left(\begin{array}{ccc} 0.8012 + 0.05287i & 0.5774 & -0.1285 - 0.07406i \\ 0.09636 - 0.354i & -0.2887 + 0.5i & -0.6317 - 0.3646i \\ 0.09636 + 0.4598i & -0.2887 - 0.5i & -0.6317 + 0.2165i \\ 0.8009 - 0.05405i & 0.5774 & -0.1285 + 0.07575i \\ 0.09596 - 0.4611i & -0.288 + 0.5i & -0.6315 - 0.2147i \\ 0.09596 + 0.353i & -0.2888 - 0.5i & -0.6315 + 0.3662i \end{array} \right) & \text{for NH,} \\ \left(\begin{array}{ccc} 0.8012 + 0.05287i & 0.5774 & -0.1285 - 0.07406i \\ 0.09636 - 0.354i & -0.2887 + 0.5i & -0.6317 - 0.3646i \\ 0.09636 + 0.4598i & -0.2887 - 0.5i & -0.6317 + 0.2165i \\ 0.8009 - 0.05405i & 0.5774 & -0.1285 + 0.07575i \\ 0.09596 - 0.4611i & -0.288 + 0.5i & -0.6315 - 0.2147i \\ 0.09596 + 0.353i & -0.2888 - 0.5i & -0.6315 + 0.3662i \end{array} \right) & \text{for IH,} \end{cases} \quad (71)$$

which are unitary and in good agreement with the constraint on the absolute values of the entries of the lepton mixing matrix given in Eq. (1).

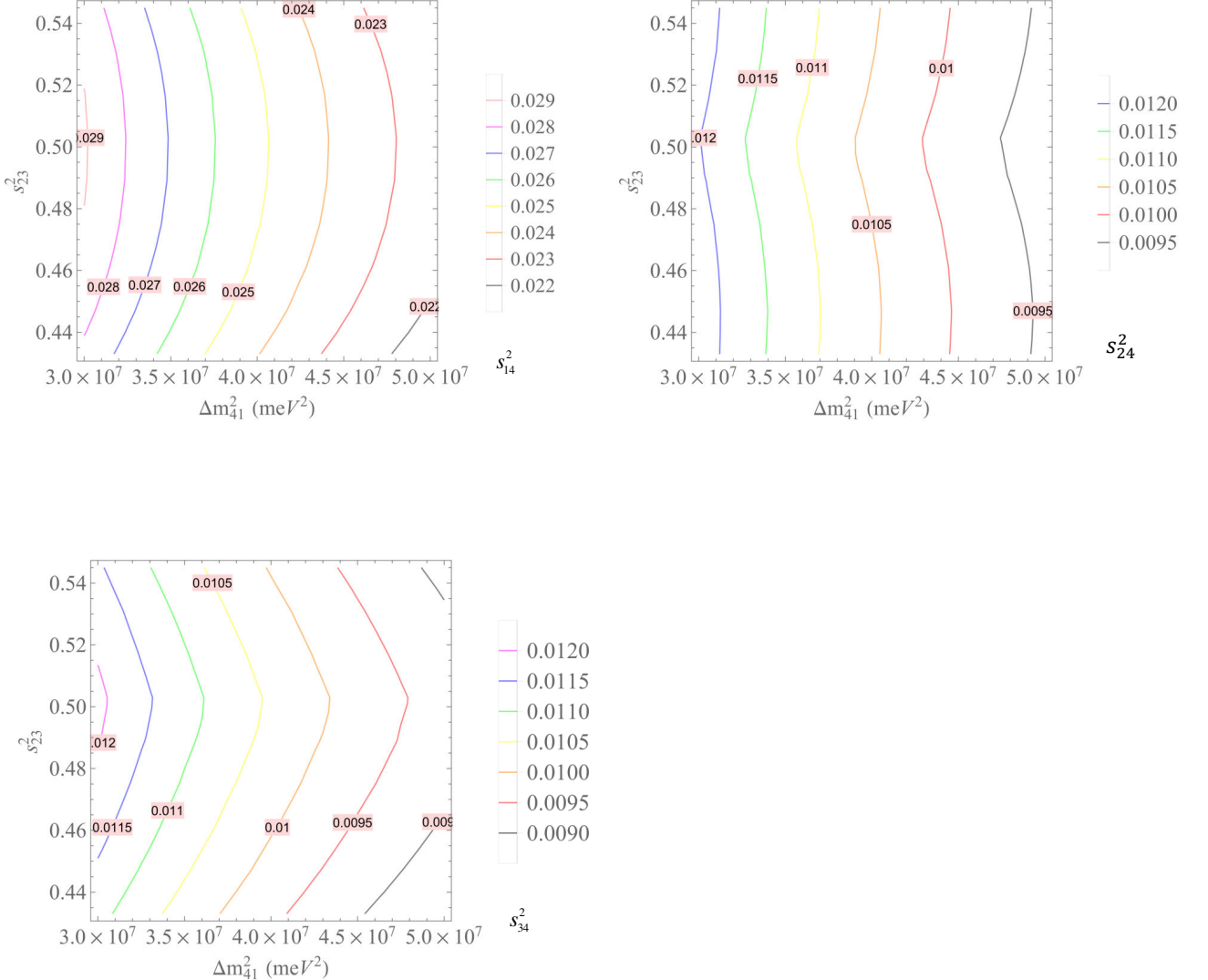


Figure 11: s_{14}^2 , s_{24}^2 and s_{34}^2 as functions of s_{23}^2 and Δm_{41}^2 with $s_{23}^2 \in (0.433, 0.545)$ and $\Delta m_{41}^2 \in (30.0, 50.0)10^6 \text{ meV}^2$ for IH.

IV. MUON ANOMALOUS MAGNETIC MOMENT

The experimental data shows a significant deviation of the muon anomalous magnetic moment from its SM value

$$\Delta a_\mu = a_\mu^{\text{exp}} - a_\mu^{\text{SM}} = (2.51 \pm 0.59) \times 10^{-9} \quad [82-89] \quad (72)$$

In this subsection, we will analyze the implications of our model in the muon anomalous magnetic moment. Muon anomalous magnetic moments mainly arises from one-loop diagrams involving the exchange of electrically neutral CP even and CP odd scalars and the muon running in the internal lines of the loop. It is worth mentioning that due to the symmetries in our model, there are no tree level flavor changing neutral scalar interaction in the leptonic Yukawa terms, thus implying that the muon is the only charged lepton contributing to the muon anomalous magnetic moment. There are also contributions arising from electrically charged scalar and right handed Majorana neutrinos but these contributions are strongly suppressed. Thus, the leading contributions to the muon anomalous magnetic

Table III: The model prediction compared to the experimental range [45, 46]

Parameters	Experimental range(NH)	Prediction(NH)	Experimental range(IH)	Prediction(IH)
$\sum_{i=1}^3 m_i(\text{meV})$	< 120	58.03 → 60.31	< 150	98.07 → 101.30
$\sin^2 \theta_{13} \times 10^2$	2.00 → 2.405	2.00 → 2.405	2.018 → 2.424	2.018 → 2.424
$\sin^2 \theta_{12}$	0.271 → 0.369	0.3401 → 0.3415	0.271 → 0.369	0.3402 → 0.3416
$\sin^2 \theta_{23}$	0.434 → 0.610	0.456 → 0.544	0.433 → 0.608	0.433 → 0.545
$\delta_{CP}(\circ)$	128 → 352	156 → 172	200 → 353	140.8 → 167.2
s_{14}^2	0.0098 → 0.0310	0.015 → 0.045	0.0098 → 0.0310	0.022 → 0.029
s_{24}^2	0.0059 → 0.0262	0.005 → 0.012	0.0059 → 0.0262	0.0095 → 0.012
s_{34}^2	0 → 0.0369	0.003 → 0.011	0 → 0.0369	0.009 → 0.012
$\langle m_{ee}^{(3)} \rangle (\text{meV})$	≈ 1.0 [95]	3.50 → 4.1	≈ 1.0 [95]	47.90 → 48.50
$m_\beta^{(3)} (\text{meV})$	8.9 → 12.6 [95]	8.85 → 9.15	8.9 → 12.6 [95]	47.17 → 49.23
$\langle m_{ee} \rangle (\text{meV})$	< 110 → 520 [74]	40.0 → 110.0	< 110 → 520 [74]	185.0 → 205.0
$m_\beta (\text{meV})$	< 1100 [96]	300.0 → 550.0	< 1100 [96]	700.0 → 900.0

Table IV: The obtained parameters

Parameters	The derived values (NH)	The derived values (IH)
k_2	-2.29	1.161
k_3	0.439	0.9758
$\cos \alpha (\alpha^\circ)$	-0.136 (97.80)	0.9758 (4.412)
k_0	5.83	0.985
$m_1(\text{meV})$	0	49.50
$m_2(\text{meV})$	8.66	50.25
$m_1(\text{meV})$	50.50	0
$\sum_{i=1}^3 m_i(\text{meV})$	59.20	99.75
$\sin \delta_{CP} (\delta_{CP}^\circ)$	-0.912 (294.0)	-0.9092 (294.60)
$m_s (\text{eV})$	2.24	4.472
s_{14}^2	0.0178	0.02853
s_{24}^2	0.00589	0.01225
s_{34}^2	0.00394	0.01157
$\langle m_{ee}^{(3)} \rangle (\text{meV})$	3.575	48.45
$\langle m_{ee} \rangle (\text{meV})$	37.27	203.90
$m_\beta^{(3)} (\text{meV})$	9.006	49.20
$m_\beta (\text{meV})$	294.20	926.40

moment take the form:

$$\Delta a_\mu \simeq \frac{\left[(y_{h\bar{\mu}_R \mu_L})^2 - (y_{h\bar{\mu}_R \mu_L}^{SM})^2 \right] m_\mu^2}{8\pi^2} I_H^{(\mu)}(m_\mu, m_h) + \frac{m_\mu^2}{8\pi^2} \left[y_{H^0 \bar{\mu}_R \mu_L}^2 I_H^{(\mu)}(m_\mu, m_{H^0}) + y_{A^0 \bar{\mu}_R \mu_L}^2 I_A^{(\mu)}(m_\mu, m_{A^0}) \right], \quad (73)$$

where the Yukawa couplings appearing in Eq. (73) are given by:

$$y_{h\bar{\mu}_R \mu_L} = \sqrt{\frac{3}{2}} (y_2 \sin \alpha - y_3 \cos \alpha), \quad y_{h\bar{\mu}_R \mu_L}^{SM} = \frac{m_\mu}{v}, \quad (74)$$

$$y_{H^0 \bar{\mu}_R \mu_L} = \sqrt{\frac{3}{2}} (y_2 \cos \alpha + y_3 \sin \alpha), \quad y_{A^0 \bar{\mu}_R \mu_L} = \sqrt{\frac{3}{2}} (y_2 \sin \beta - y_3 \cos \beta), \quad (75)$$

whereas the loop function $I_{H(A)}^{(\mu)}(m_f, m_{H,A})$ has the form [90–94]:

$$I_{H(A)}^{(\mu)}(m_f, m_{H,A}) = \int_0^1 \frac{x^2 \left(1 - x \pm \frac{m_f}{m_\mu} \right)}{m_\mu^2 x^2 + (m_f^2 - m_\mu^2)x + m_{H,A}^2 (1-x)} dx. \quad (76)$$

Figure 12 shows the allowed parameter space in the $m_{H^0} - m_{A^0}$ plane consistent with the muon anomalous magnetic moment. We find that our model can successfully accommodate the experimental values of the muon anomalous magnetic moment.

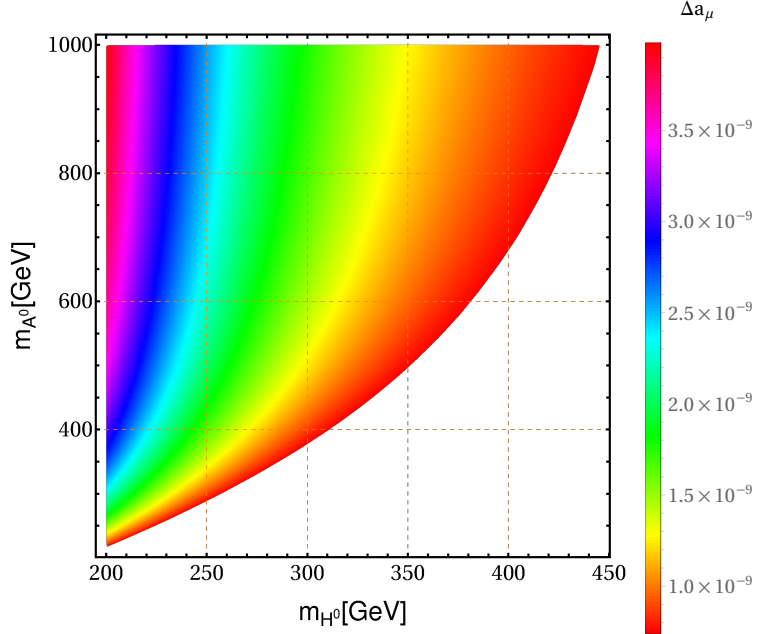


Figure 12: Allowed parameter space in the $m_{H^0} - m_{A^0}$ plane consistent with the muon anomalous magnetic moment.

V. CONCLUSIONS

We have proposed a $B-L$ model combined with the $S_4 \times Z_3 \times Z_4$ discrete group which successfully explains the recent $3+1$ sterile-active neutrino data. The tiny masses of the light active neutrinos are obtained through the type-I seesaw mechanism. The active-active and sterile-active neutrino mixing angles are predicted to be consistent with the recent constraints where 0.3401 (0.3402) $\leq \sin^2 \theta_{12} \leq 0.3415$ (0.3416), 0.456 (0.433) $\leq \sin^2 \theta_{23} \leq 0.544$ (0.545), 2.00 (2.018) $\leq 10^2 \times \sin^2 \theta_{13} \leq 2.405$ (2.424), 156 (140.8) $\leq \delta_{CP}^{(\circ)} \leq 172$ (167.2) for normal (inverted) ordering of the three neutrino scenario, and 0.015 (0.022) $\leq s_{14}^2 \leq 0.045$ (0.029), 0.005 (0.0095) $\leq s_{24}^2 \leq 0.012$ (0.012), 0.003 (0.009) $\leq s_{34}^2 \leq 0.011$ for normal (inverted) ordering of the $3+1$ neutrino scenario. The effective neutrino masses are predicted to be in the ranges 40.0 (185) $\leq \langle m_{ee} \rangle [\text{meV}] \leq 110.0$ (205.0) and 300 (700) $\leq \langle m_\beta \rangle [\text{meV}] \leq 550$ (900), for normal and inverted neutrino mass orderings, respectively, range of values consistent with the recent experimental data. Our model predicts flavour conserving leptonic neutral scalar interactions and successfully explains the muon $g-2$ anomaly.

Acknowledgments

A.E.C.H is supported by ANID-Chile FONDECYT 1210378, ANID PIA/APOYO AFB180002 and ANID- Programa Milenio - code ICN2019_044. H. N. Long acknowledges the financial support of the International Centre of Physics at the Institute of Physics, VAST under grant No: ICP.2022.02.

Appendix A: Forbidden terms

Table V: Forbidden terms

Couplings	Forbidden by
$(\bar{\psi}_L \psi_L^c)_1 \tilde{H}^2, (\bar{\psi}_L \psi_L^c)_1 \tilde{H'}^2, (\bar{\nu}_R^C \nu_R)_1 (\chi^{*2})_1, (\bar{\nu}_R^C \nu_R)_1 (\phi \varphi^*)_1, (\bar{\nu}_R^C \nu_R)_2 (\phi \varphi^*)_2,$ $(\bar{\nu}_R^C \nu_R)_3 (\phi \varphi^*)_3, (\bar{\nu}_R^C \nu_R)_{3'} (\phi \varphi^*)_{3'}, (\bar{\nu}_R^C \nu_R)_3 (\phi \rho^*)_3, (\bar{\nu}_R^C \nu_R)_1 (\phi^* \phi_s)_1,$ $(\bar{\nu}_R^C \nu_R)_2 (\phi^* \phi_s)_2, (\bar{\nu}_R^C \nu_R)_3 (\phi^* \phi_s)_3, (\bar{\nu}_R^C \nu_R)_{3'} (\phi^* \phi_s)_{3'}, (\bar{\nu}_R^C \nu_R)_1 (\phi \phi_s^*)_1,$ $(\bar{\nu}_R^C \nu_R)_2 (\varphi \phi_s^*)_2, (\bar{\nu}_R^C \nu_R)_3 (\varphi \phi_s^*)_3, (\bar{\nu}_R^C \nu_R)_{3'} (\varphi \phi_s^*)_{3'}, (\bar{\nu}_R^C \nu_R)_1 (\rho \phi_s^*)_1, (\bar{\nu}_s^C \nu_R)_3 \varphi,$ $(\bar{\nu}_s^C \nu_R)_3 (\phi \chi^*)_3, (\bar{\nu}_s^C \nu_s)_1 (\phi^2)_1, (\bar{\nu}_s^C \nu_s)_1 (\phi^{*2})_1, (\bar{\nu}_s^C \nu_s)_1 (\phi^* \varphi^*)_1, (\bar{\nu}_s^C \nu_s)_1 (\varphi \phi_s)_1.$ $(\bar{\psi}_L l_{1R})_3 (H' \phi)_{3'}, (\bar{\psi}_L \nu_R)_1 (\tilde{H}' \rho)_{1'}.$	$U(1)_{B-L}$
$(\bar{\psi}_L l_{1R})_3 (H \varphi)_3, (\bar{\psi}_L l_{1R})_3 (H \phi_s)_3, (\bar{\psi}_L l_{\alpha R})_3 (H \varphi)_3, (\bar{\psi}_L l_{\alpha R})_3 (H \phi_s)_3,$ $(\bar{\psi}_L l_{\alpha R})_3 (H' \varphi)_{3'}, (\bar{\psi}_L l_{\alpha R})_3 (H' \phi_s)_{3'}, (\bar{\psi}_L \nu_R)_3 (\tilde{H} \phi)_3, (\bar{\psi}_L \nu_R)_3 (\tilde{H} \phi_s)_3,$ $(\bar{\psi}_L \nu_R)_{3'} (\tilde{H}' \phi)_{3'}, (\bar{\psi}_L \nu_R)_{3'} (\tilde{H}' \phi_s)_{3'}, (\bar{\nu}_s^C \nu_R)_3 (\phi \chi)_3, (\bar{\nu}_s^C \nu_R)_3 (\varphi \chi)_3.$	S_4
$(\bar{\psi}_L l_{\alpha R})_3 (H' \phi_s^*)_{3'}, (\bar{\psi}_L \nu_R)_1 \tilde{H}, (\bar{\psi}_L \nu_R)_3 (\tilde{H} \varphi^*)_3, (\bar{\psi}_L \nu_R)_1 (\tilde{H} \rho^*)_1,$ $(\bar{\psi}_L \nu_R)_{3'} (\tilde{H}' \varphi^*)_{3'}, (\bar{\psi}_L \nu_s)_3 (\tilde{H} \phi^*)_3, (\bar{\psi}_L \nu_s)_3 (\tilde{H} \phi_s)_3, (\bar{\nu}_R^C \nu_R)_3 (\varphi \chi)_3,$ $(\bar{\nu}_R^C \nu_R)_3 (\varphi^* \chi)_3, (\bar{\nu}_R^C \nu_R)_1 (\rho \chi)_1, (\bar{\nu}_R^C \nu_R)_1 (\rho^* \chi)_1, (\bar{\nu}_s^C \nu_R)_3 (\phi^* \chi)_3.$	Z_3
$(\bar{\psi}_L l_{\alpha R})_3 (H' \phi_s^*)_{3'}, (\bar{\psi}_L \nu_R)_1 \tilde{H}, (\bar{\psi}_L \nu_R)_3 (\tilde{H} \varphi^*)_3, (\bar{\psi}_L \nu_R)_1 (\tilde{H} \rho^*)_1,$ $(\bar{\psi}_L \nu_R)_{3'} (\tilde{H}' \varphi^*)_{3'}, (\bar{\psi}_L \nu_s)_3 (\tilde{H} \phi^*)_3, (\bar{\psi}_L \nu_s)_3 (\tilde{H} \phi_s)_3, (\bar{\nu}_R^C \nu_R)_3 (\varphi \chi)_3,$ $(\bar{\nu}_R^C \nu_R)_3 (\varphi^* \chi)_3, (\bar{\nu}_R^C \nu_R)_1 (\rho \chi)_1, (\bar{\nu}_R^C \nu_R)_1 (\rho^* \chi)_1, (\bar{\nu}_s^C \nu_R)_3 (\phi^* \chi)_3.$	Z_4

Appendix B: Higgs potential invariant under Γ symmetry

The total renormalizable scalar potential invariant under Γ symmetry is given by⁴:

$$\begin{aligned}
V_{\text{scal}} = & V(H) + V(H') + V(\phi) + V(\varphi) + V(\rho) + V(\chi) + V(\phi_s) + V(HH') + V(H\phi) \\
& + V(H\varphi) + V(H\rho) + V(H\chi) + V(H\phi_s) + V(H'\phi) + V(H'\varphi) + V(H'\rho) + V(H'\chi) \\
& + V(H'\phi_s) + V(\phi\varphi) + V(\phi\rho) + V(\phi\chi) + V(\phi\phi_s) + V(\varphi\rho) + V(\varphi\chi) + V(\varphi\phi_s) \\
& + V(\rho\chi) + V(\rho\phi_s) + V(\chi\phi_s) + V_{\text{trip}} + V_{\text{quart}},
\end{aligned} \tag{B1}$$

where

$$\begin{aligned}
V(H) &= \mu_H^2 H^\dagger H + \lambda^H (H^\dagger H)^2, \quad V(H') = V(H, H \rightarrow H'), \\
V(\phi) &= \mu_\phi^2 \phi^* \phi + \lambda_1^\phi (\phi^* \phi)_1 (\phi^* \phi)_1 + \lambda_2^\phi (\phi^* \phi)_2 (\phi^* \phi)_2 + \lambda_3^\phi (\phi^* \phi)_3 (\phi^* \phi)_3 + \lambda_4^\phi (\phi^* \phi)_{3'} (\phi^* \phi)_{3'}, \\
V(\varphi) &= V(\phi \rightarrow \varphi), \quad V(\rho) = \mu_\rho^2 \rho^* \rho + \lambda^\rho (\rho^* \rho)_1 (\rho^* \rho)_1, \quad V(\chi) = V(\rho \rightarrow \chi), \quad V(\phi_s) = V(\phi \rightarrow \phi_s), \\
V(H, H') &= \lambda_1^{HH'} (H^\dagger H)_1 (H'^\dagger H')_1 + \lambda_2^{HH'} (H^\dagger H')_1' (H'^\dagger H)_1', \quad V(H, \phi) = \lambda_1^{H\phi} (H^\dagger H)_1 (\phi^* \phi)_1 \\
& + \lambda_2^{H\phi} (H^\dagger \phi)_3 (\phi^* H)_3, \quad V(H, \varphi) = V(H, \phi \rightarrow \varphi), \quad V(H, \rho) = \lambda_1^{H\rho} (H^\dagger H)_1 (\rho^* \rho)_1 \\
& + \lambda_2^{H\rho} (H^\dagger \rho)_1 (\rho^* H)_1, \quad V(H, \chi) = V(H, \rho \rightarrow \chi), \quad V(H, \phi_s) = V(H, \phi \rightarrow \phi_s),
\end{aligned}$$

⁴ Here, $V(a_1 \rightarrow a_2, b_1 \rightarrow b_2, \dots) \equiv V(a_1, b_1, \dots)|_{\{a_1=a_2, b_1=b_2, \dots\}}$.

$$\begin{aligned}
V(H, H') &= \lambda_1^{HH'}(H^\dagger H)_1(H'^\dagger H')_1 + \lambda_2^{HH'}(H^\dagger H')_{1'}(H'^\dagger H)_{1'}, V(H, \phi) = \lambda_1^{H\phi}(H^\dagger H)_1(\phi^*\phi)_1 \\
&\quad + \lambda_2^{H\phi}(H^\dagger \phi)_3(\phi^* H)_3, \quad V(H, \varphi) = V(H, \phi \rightarrow \varphi), \quad V(H, \rho) = \lambda_1^{H\rho}(H^\dagger H)_1(\rho^*\rho)_1 \\
&\quad + \lambda_2^{H\rho}(H^\dagger \rho)_1(\rho^* H)_1, \quad V(H, \chi) = V(H, \rho \rightarrow \chi), \quad V(H, \phi_s) = V(H, \phi \rightarrow \phi_s), \\
V(H', \phi) &= \lambda_1^{H'\phi}(H'^\dagger H')_1(\phi^*\phi)_1 + \lambda_2^{H'\phi}(H'^\dagger \phi)_{3'}(\phi^* H')_{3'}, \quad V(H', \varphi) = V(H', \phi \rightarrow \varphi), \\
V(H', \rho) &= \lambda_1^{H'\rho}(H'^\dagger H')_1(\rho^*\rho)_1 + \lambda_2^{H'\rho}(H'^\dagger \rho)_{1'}(\rho^* H')_{1'}, \quad V(H', \chi) = V(H', \rho \rightarrow \chi), \\
V(H', \phi_s) &= V(H', \phi \rightarrow \phi_s), \quad V(\phi, \rho) = \lambda_1^{\phi\rho}(\phi^*\phi)_1(\rho^*\rho)_1 + \lambda_2^{\phi\rho}(\phi^*\rho)_3(\rho^*\phi)_3, \\
V(\phi, \chi) &= V(\phi, \rho \rightarrow \chi), \quad V(\phi, \varphi) = \lambda_1^{\phi\varphi}(\phi^*\phi)_1(\varphi^*\varphi)_1 + \lambda_2^{\phi\varphi}(\phi^*\phi)_2(\varphi^*\varphi)_2 + \lambda_3^{\phi\varphi}(\phi^*\phi)_3(\varphi^*\varphi)_3 \\
&\quad + \lambda_4^{\phi\varphi}(\phi^*\phi)_{3'}(\varphi^*\varphi)_{3'}, \quad \lambda_5^{\phi\varphi}(\phi^*\varphi)_1(\varphi^*\phi)_1 + \lambda_6^{\phi\varphi}(\phi^*\varphi)_2(\varphi^*\phi)_2 + \lambda_7^{\phi\varphi}(\phi^*\varphi)_3(\varphi^*\phi)_3 \\
&\quad + \lambda_8^{\phi\varphi}(\phi^*\varphi)_{3'}(\varphi^*\phi)_{3'}, \quad V(\phi, \phi_s) = V(\phi, \varphi \rightarrow \phi_s), \quad V(\varphi, \chi) = V(\phi \rightarrow \varphi, \chi), \\
V(\varphi, \phi_s) &= V(\phi \rightarrow \varphi, \phi_s), \quad V(\rho, \chi) = \lambda_1^{\rho\chi}(\rho^*\rho)_1(\chi^*\chi)_1 + \lambda_2^{\rho\chi}(\rho^*\chi)_1(\chi^*\rho)_1, \\
V(\rho, \phi_s) &= V(H \rightarrow \rho, \phi \rightarrow \phi_s), \quad V(\chi, \phi_s) = V(\rho \rightarrow \chi, \phi_s), \\
V_{\text{trip}} &= \lambda_1^{\phi\varphi\rho}(\phi^*\phi)_3(\varphi^*\rho)_3 + \lambda_2^{\phi\varphi\rho}(\phi^*\phi)_3(\varphi\rho^*)_3 + \lambda_3^{\phi\varphi\rho}(\phi^*\rho)_3(\varphi^*\phi)_3 + \lambda_4^{\phi\varphi\rho}(\phi^*\varphi)_3(\phi\rho^*)_3, \\
V_{\text{quart}} &= \lambda_1^{\phi\varphi\rho\phi_s}(\phi\varphi)_3(\rho\phi_s)_3 + \lambda_2^{\phi\varphi\rho\phi_s}(\phi\phi_s)_3(\rho\varphi)_3 + \lambda_3^{\phi\varphi\rho\phi_s}(\phi_s\varphi)_3(\rho\phi)_3 \\
&\quad + \lambda_4^{\phi\varphi\rho\phi_s}(\phi^*\varphi)_3(\rho^*\phi_s)_3 + \lambda_5^{\phi\varphi\rho\phi_s}(\phi^*\phi_s)_3(\rho^*\varphi^*)_3 + \lambda_6^{\phi\varphi\rho\phi_s}(\phi_s^*\varphi^*)_3(\rho^*\phi^*)_3. \tag{B2}
\end{aligned}$$

Now we show that the VEV alignments in Eq. (3) satisfy the minimization condition of the scalar potential V_{scal} of the model whose explicit expression is given in Eqs. (B1)-(B2). For this purpose we suppose that the VEVs of the scalars H, H', ϕ, ρ, χ and ϕ_s are real while that of φ is complex, i.e., $v^* = v$, $v'^* = v'$, $v_\phi^* = v_\phi$, $v_\rho^* = v_\rho$, $v_\chi^* = v_\chi$, $v_{\phi_s}^* = v_{\phi_s}$ and $v_\varphi = v_0 e^{i\alpha}$. The minimization condition of V_{scal} reads

$$\frac{\partial V_{\text{scal}}}{\partial v_\lambda} = 0, \quad \delta_\lambda^2 \sim \frac{\partial^2 V_{\text{scal}}}{\partial v_\lambda^2} > 0 \quad (v_\lambda = v, v', v_\phi, v_\rho, v_\chi, v_{\phi_s}, v_0, \alpha). \tag{B3}$$

For simplicity we will work with the following benchmark points:

$$\begin{aligned}
\lambda_1^{H\varphi} &= \lambda_2^{H\varphi} = \lambda_1^{H'\varphi} = \lambda_2^{H'\varphi} = \lambda_1^{H\chi} = \lambda_2^{H\chi} = \lambda_1^{H'\chi} = \lambda_2^{H'\chi} = \lambda_1^{HH'} = \lambda_2^{HH'} \\
&= \lambda_1^{H\phi} = \lambda_2^{H\phi} = \lambda_1^{H'\phi} = \lambda_2^{H'\phi} = \lambda_1^{H\rho} = \lambda_2^{H\rho} = \lambda_1^{H'\rho} = \lambda_2^{H'\rho} = \lambda_1^{H\phi_s} = \lambda_2^{H\phi_s} \\
&= \lambda_1^{H'\phi_s} = \lambda_2^{H'\phi_s} = \lambda_1^{\phi\chi} = \lambda_2^{\phi\chi} = \lambda_1^{\phi\varphi} = \lambda_2^{\phi\varphi} = \lambda_5^{\phi\varphi} = \lambda_6^{\phi\varphi} = \lambda_7^{\phi\varphi} = \lambda_8^{\phi\varphi} = \lambda_1^{H'\phi} = \lambda_2^{H'\phi} \\
&= \lambda_1^{\phi\rho} = \lambda_2^{\phi\rho} = \lambda_1^{\phi\phi_s} = \lambda_3^{\phi\phi_s} = \lambda_5^{\phi\phi_s} = \lambda_6^{\phi\phi_s} = \lambda_7^{\phi\phi_s} = \lambda_8^{\phi\phi_s} = \lambda_1^{\varphi\chi} = \lambda_2^{\varphi\chi} = \lambda_1^{\varphi\rho} \\
&= \lambda_2^{\varphi\rho} = \lambda_1^{\rho\chi} = \lambda_2^{\rho\chi} = \lambda_1^{\rho\phi_s} = \lambda_2^{\rho\phi_s} = \lambda_1^{H\chi} = \lambda_2^{H\chi} = \lambda_1^{X\phi_s} = \lambda_2^{X\phi_s} = \lambda_1^{\varphi\phi_s} = \lambda_2^{\varphi\phi_s} \\
&= \lambda_7^{\varphi\phi_s} = \lambda_8^{\varphi\phi_s} = \lambda_3^{\phi\varphi\rho\phi_s} = \lambda_2^{\phi\varphi\rho\phi_s} = \lambda_1^{\phi\varphi\rho\phi_s} = \lambda_3^{\phi\varphi\rho} = \lambda_1^{\phi\varphi\rho} = \lambda^x, \tag{B4}
\end{aligned}$$

$$\lambda_6^{\phi\varphi\rho\phi_s} = \lambda_5^{\phi\varphi\rho\phi_s} = \lambda_4^{\phi\varphi\rho\phi_s} = a\lambda_1^{\phi\varphi\rho\phi_s} = a\lambda^x, \quad \lambda_4^{\phi\varphi\rho} = \lambda_2^{\phi\varphi\rho} = a\lambda^x, \tag{B5}$$

$$\lambda_1^\phi = \lambda_3^\phi = \lambda^\phi, \quad \lambda_1^\varphi = \lambda_2^\varphi = \lambda^\varphi, \quad \lambda_1^{\phi_s} = \lambda_2^{\phi_s} = \lambda_3^{\phi_s} = \lambda^{\phi_s}. \tag{B6}$$

As a consequence, the condition (B3) becomes

$$\mu_H^2 + 2\lambda^H v^2 + 2\lambda^x (v_\varphi^2 + v_\chi^2 + v'^2 + 3v_\phi^2 + v_\rho^2 + 2v_s^2) = 0, \quad (\text{B7})$$

$$\mu_{H'}^2 + 2\lambda^{H'} v'^2 + 2\lambda^x (v^2 + v_\varphi^2 + v_\chi^2 + 3v_\phi^2 + v_\rho^2 + 2v_s^2) = 0, \quad (\text{B8})$$

$$6\mu_\phi^2 v_\phi + 84\lambda^\phi v_\phi^3 + 2\lambda^x [6v_\phi(v^2 + v_\varphi^2 + v_\chi^2 + v'^2 + v_\rho^2) + 20v_\phi v_s^2 + e^{i\alpha} v_\varphi v_\rho (4av_\phi + 3av_s) + e^{-i\alpha} v_\varphi v_\rho (4v_\phi + 3av_s)] = 0, \quad (\text{B9})$$

$$\mu_\varphi^2 v_\varphi + 6\lambda^\varphi v_\varphi^3 + \lambda^x [2v_\varphi(v^2 + v_\chi^2 + v'^2 + 3v_\phi^2 + v_\rho^2) + e^{i\alpha} v_\phi v_\rho (2av_\phi + 3av_s) + e^{-i\alpha} v_\phi v_\rho (2v_\phi + 3av_s)] = 0, \quad (\text{B10})$$

$$v_\rho [\mu_\rho^2 + 2\lambda^\rho v_\rho^2 + 2\lambda^x (v^2 + v_\varphi^2 + v_\chi^2 + v'^2 + 3v_\phi^2 + 2v_s^2)] + e^{i\alpha} \lambda^x v_\varphi v_\phi (2av_\phi + 3av_s) + e^{-i\alpha} \lambda^x v_\varphi v_\phi (2av_\phi + 3av_s) = 0, \quad (\text{B11})$$

$$\mu_\chi^2 + 2\lambda^\chi v_\chi^2 + 2\lambda^x (v^2 + v_\varphi^2 + v'^2 + 3v_\phi^2 + v_\rho^2 + 2v_s^2) = 0, \quad (\text{B12})$$

$$3\lambda^x v_\varphi v_\phi v_\rho (ae^{-i\alpha} + e^{i\alpha}) + 2v_s [\mu_\phi^2 + 2\lambda^x (v^2 + v_\chi^2 + v'^2 + 5v_\phi^2 + v_\rho^2) + 10\lambda^{\phi_s} v_s^2] = 0, \quad (\text{B13})$$

$$e^{2i\alpha} (2av_\phi + 3av_s) - 2v_\phi - 3av_s = 0, \quad (\text{B14})$$

$$\mu_H^2 + 6\lambda^H v^2 + 2\lambda^x (v_\varphi^2 + v_\chi^2 + v'^2 + 3v_\phi^2 + v_\rho^2 + 2v_s^2) > 0, \quad (\text{B15})$$

$$\mu_{H'}^2 + 6\lambda^{H'} v'^2 + 2\lambda^x (v_\varphi^2 + v_\chi^2 + v^2 + 3v_\phi^2 + v_\rho^2 + 2v_s^2) > 0, \quad (\text{B16})$$

$$3\mu_\phi^2 + 126\lambda^\phi v_\phi^2 + 4\lambda^x v_\varphi v_\rho (e^{-i\alpha} + be^{i\alpha}) + 6\lambda^x (v^2 + v_\varphi^2 + v_\chi^2 + v'^2 + v_\rho^2) + 20\lambda^x v_s^2 > 0, \quad (\text{B17})$$

$$\mu_\varphi^2 + 18\lambda^\varphi v_\varphi^2 + 2\lambda^x (v^2 + v_\chi^2 + v'^2 + 3v_\phi^2 + v_\rho^2) > 0, \quad (\text{B18})$$

$$\mu_\rho^2 + 6\lambda^\rho v_\rho^2 + 2\lambda^x (v^2 + v_\varphi^2 + v_\chi^2 + v'^2 + 3v_\phi^2 + 2v_s^2) > 0, \quad (\text{B19})$$

$$\mu_\chi^2 + 6\lambda^\chi v_\chi^2 + 2\lambda^x (v^2 + v_\varphi^2 + v'^2 + 3v_\phi^2 + v_\rho^2 + 2v_s^2) > 0, \quad (\text{B20})$$

$$\mu_{\phi_s}^2 + 2\lambda^x (v^2 + v_\chi^2 + v'^2 + 5v_\phi^2 + v_\rho^2) + 30\lambda^{\phi_s} v_s^2 > 0, \quad (\text{B21})$$

$$-2v_\phi - 3av_s - e^{2i\alpha} (2av_\phi + 3av_s) > 0. \quad (\text{B22})$$

The system of Eqs. (B7)-(B14) yields the following solution:

$$\begin{aligned} \lambda^H &= -\frac{\mu_H^2 + 2\lambda^x (v_\varphi^2 + v_\chi^2 + v'^2 + 3v_\phi^2 + v_\rho^2 + 2v_s^2)}{2v^2}, \\ \lambda^{H'} &= -\frac{\mu_{H'}^2 + 2\lambda^x (v_\varphi^2 + v_\chi^2 + v^2 + 3v_\phi^2 + v_\rho^2 + 2v_s^2)}{2v'^2}, \\ \lambda^\phi &= -\frac{1}{42v_\phi^3} \left[(3\mu_\phi^2 + 6\lambda^x v^2 + 6\lambda^x v_\varphi^2 + 6\lambda^x v_\chi^2 + 6\lambda^x v'^2 + 6\lambda^x v_\rho^2 + 20\lambda^x v_s^2) v_\phi \right. \\ &\quad \left. + \lambda^x v_\varphi v_\rho \left(\frac{(4av_\phi + 3av_s)\sqrt{2v_\phi + 3av_s}}{\sqrt{2av_\phi + 3v_s}} + \frac{\sqrt{2av_\phi + 3v_s}(4v_\phi + 3av_s)}{\sqrt{2v_\phi + 3av_s}} \right) \right], \\ \lambda^\varphi &= -\frac{\mu_\varphi^2 v_\varphi + 2\lambda^x [v_\varphi(v^2 + v_\chi^2 + v'^2 + 3v_\phi^2 + v_\rho^2) + v_\phi v_\rho \sqrt{(2av_\phi + 3av_s)(2v_\phi + 3av_s)}]}{6v_\varphi^3}, \\ \lambda^\rho &= -\frac{\mu_\rho^2 v_\rho + 2\lambda^x [v_\rho(v^2 + v_\varphi^2 + v_\chi^2 + v'^2 + 3v_\phi^2 + 2v_s^2) + v_\varphi v_\phi \sqrt{(2av_\phi + 3av_s)(2v_\phi + 3av_s)}]}{2v_\rho^3}, \\ \lambda^\chi &= -\frac{\mu_\chi^2 + 2\lambda^x (v^2 + v_\varphi^2 + v'^2 + 3v_\phi^2 + v_\rho^2 + 2v_s^2)}{2v_\chi^2}, \quad \alpha = i \log \left(\sqrt{\frac{2av_\phi + 3av_s}{2v_\phi + 3av_s}} \right), \\ \lambda^{\phi_s} &= -\frac{\mu_{\phi_s}^2 v_s + 2\lambda^x (v^2 + v_\chi^2 + v'^2 + 5v_\phi^2 + v_\rho^2) v_s}{10v_s^3} - \frac{3\lambda^x v_\varphi v_\phi v_\rho (v_\phi + a^2 v_\phi + 3av_s)}{10v_s^3 \sqrt{(2av_\phi + 3av_s)(2v_\phi + 3av_s)}}. \end{aligned} \quad (\text{B23})$$

With the aid of the solution (B23), expressions (B15)-(B18) become

$$\delta_v^2 \sim -\mu_H^2 - 2\lambda^x (v_\varphi^2 + v_\chi^2 + v'^2 + 3v_\phi^2 + v_\rho^2 + 2v_s^2) > 0, \quad (\text{B24})$$

$$\delta_{v'}^2 \sim -\mu_{H'}^2 - 2\lambda^x (v_\varphi^2 + v_\chi^2 + v^2 + 3v_\phi^2 + v_\rho^2 + 2v_s^2) > 0, \quad (\text{B25})$$

$$\begin{aligned} \delta_\phi^2 \sim & -3\mu_\phi^2 - \lambda^x [6v^2 + 6v_\varphi^2 + 6(v_\chi^2 + v'^2 + v_\rho^2) + 20v_s^2 \\ & + \frac{v_\varphi v_\rho [av_\phi(21av_s + 16v_\phi) + 3v_s(9av_s + 7v_\phi)]}{v_\phi \sqrt{3av_s + 2v_\phi} \sqrt{2av_\phi + 3v_s}}] > 0, \end{aligned} \quad (\text{B26})$$

$$\delta_\varphi^2 \sim -\mu_\varphi^2 - 2\lambda^x (v^2 + v_\chi^2 + v'^2 + 3v_\phi^2 + v_\rho^2) - \frac{3\lambda^x v_\phi v_\rho \sqrt{(2av_\phi + 3v_s)(2v_\phi + 3av_s)}}{v_\varphi} > 0, \quad (\text{B27})$$

$$\delta_\rho^2 \sim -\mu_\rho^2 - 2\lambda^x (v^2 + v_\chi^2 + v'^2 + 3v_\phi^2 + v_\varphi^2) - \frac{3\lambda^x v_\phi v_\varphi \sqrt{(2av_\phi + 3v_s)(2v_\phi + 3av_s)}}{v_\rho} > 0, \quad (\text{B28})$$

$$\delta_\chi^2 = -\mu_\chi^2 - 2\lambda^x (v^2 + v_\varphi^2 + v'^2 + 3v_\phi^2 + v_\rho^2 + 2v_s^2) > 0, \quad (\text{B29})$$

$$\delta_{\phi_s}^2 \sim -2\mu_{\phi_s}^2 - 4\lambda^x (v^2 + v_\chi^2 + v'^2 + 5v_\phi^2 + v_\rho^2) - \frac{9\lambda^x v_\varphi v_\phi v_\rho (v_\phi + a^2 v_\phi + 3av_s)}{v_s \sqrt{(2av_\phi + 3v_s)(2v_\phi + 3av_s)}} > 0,$$

$$\delta_\alpha^2 \sim -\lambda^x v_\varphi v_\phi v_\rho \sqrt{3av_s + 2v_\phi} \sqrt{2av_\phi + 3v_s} > 0. \quad (\text{B30})$$

Assuming that $\mu_H^2, \mu_{H'}^2, \mu_\phi^2, \mu_\varphi^2, \mu_\rho^2, \mu_\chi^2$ and $\mu_{\phi_s}^2$ are negative and of the same order of magnitude and the same as that of the SM [61]⁵,

$$\mu_H^2 \sim \mu_{H'}^2 \sim \mu_\phi^2 \sim \mu_\varphi^2 \sim \mu_\rho^2 \sim \mu_\chi^2 \sim \mu_{\phi_s}^2 \sim -10^4 \text{ GeV}. \quad (\text{B31})$$

Expressions Eqs. (4), (5), (B25)-(B30) and (B31) tell us that $\delta_v^2 = \delta_{v'}^2$ and δ_χ^2 depend on one parameter λ^x while $\delta_\phi^2, \delta_\varphi^2, \delta_\rho^2, \delta_{\phi_s}^2$ and δ_α^2 depend on two parameters λ^x and a which are respectively plotted in Figs. 13 and 14 with $\lambda^x \in (-10^{-2}, -10^{-4})$ and $a \in (1.0, 5.0)$. These figures imply that the expressions (B25)–(B30) are always satisfied by the VEV alignments in Eq. (3).

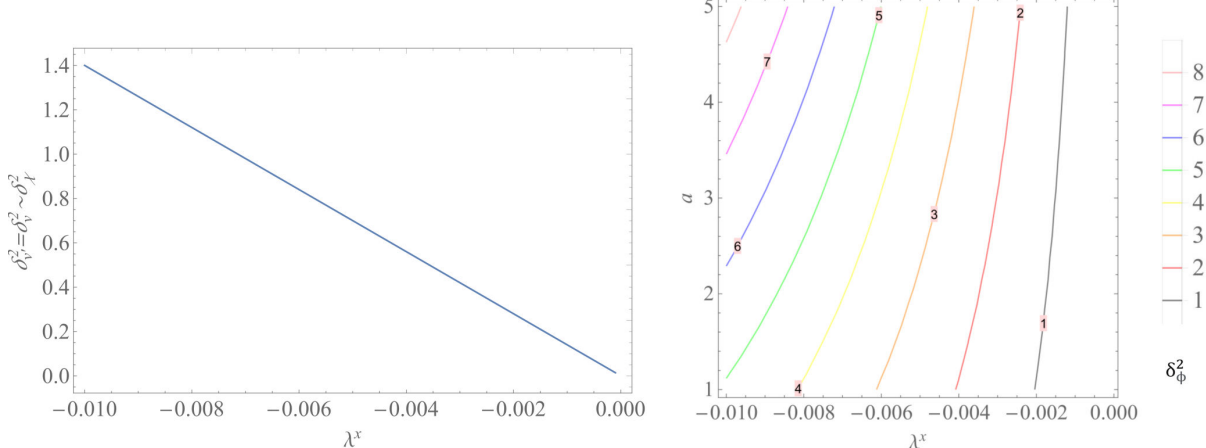


Figure 13: $\delta_v^2 = \delta_{v'}^2 \simeq \delta_\chi^2$ versus λ^x (in the left panel), and δ_ϕ^2 versus λ^x and a (in the right panel) with $\lambda^x \in (-10^{-2}, -10^{-4})$ and $a \in (1.0, 5.0)$

⁵ In the SM [61], $|\mu| = 88.4$ GeV. Here, we use $|\mu_H| \sim |\mu_\phi| \sim |\mu_l| \sim |\mu_\nu| = 10^2$ GeV for their scales.

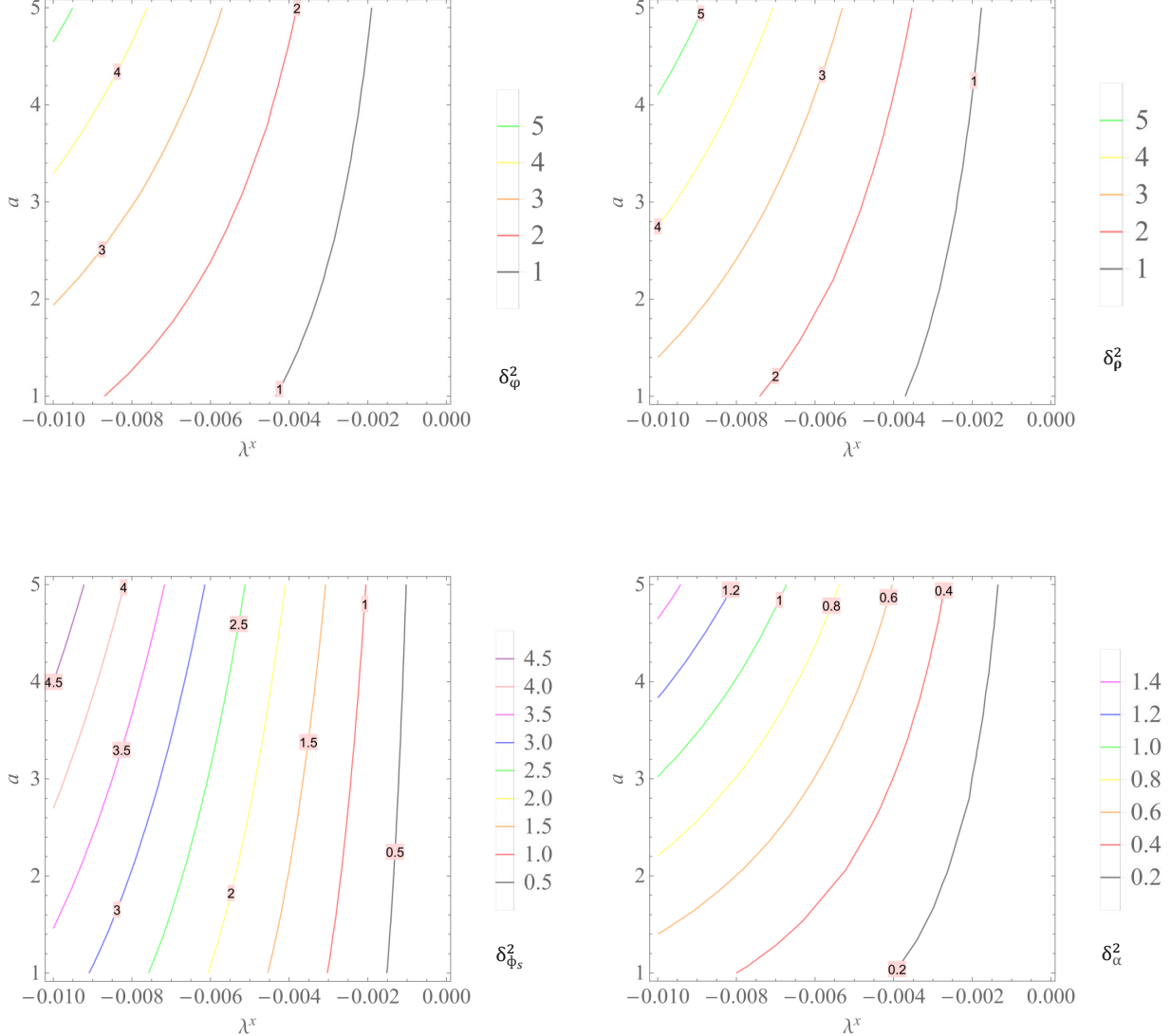


Figure 14: δ_φ^2 (upper left), δ_ρ^2 (upper right), $\delta_{\phi_s}^2$ (bottom left) and δ_α^2 (bottom right) versus λ^x and a with $\lambda^x \in (-10^{-2}, -10^{-4})$ and $a \in (1.0, 5.0)$

Appendix C: The dependence of $|U_{ij}|$ ($i = 1, 2, 3; j = 1, 3$) on s_{13} and s_{23} for normal hierarchy

Appendix D: The dependence of $|U_{ij}|$ ($i = 1, 2, 3; j = 1, 3$) on s_{13} and s_{23} for inverted hierarchy

-
- [1] A. A. Aguilar-Arevalo *et al.* [MiniBooNE Collaboration], *Event Excess in the MiniBooNE Search for $\bar{\nu}_\mu \rightarrow \bar{\nu}_e$ Oscillations*, Phys. Rev. Lett. 105 (2010) 181801. <https://doi.org/10.1103/PhysRevLett.105.181801>.
- [2] A. A. Aguilar-Arevalo *et al.* [MiniBooNE Collaboration], *Improved Search for $\bar{\nu}_\mu \rightarrow \bar{\nu}_e$ Oscillations in the MiniBooNE Experiment*, Phys. Rev. Lett. 110 (2013) 161801. <https://doi.org/10.1103/PhysRevLett.110.161801>.
- [3] K. Abe *et al.* [Super-Kamiokande Collaboration], *Limits on sterile neutrino mixing using atmospheric neutrinos in Super-Kamiokande*, Phys. Rev. D 91 (2015) 052019. <https://doi.org/10.1103/PhysRevD.91.052019>.
- [4] A. A. Aguilar-Arevalo *et al.* [MiniBooNE Collaboration], *Significant Excess of Electronlike Events in the MiniBooNE Short-Baseline Neutrino Experiment*, Phys. Rev. Lett. 121 (2018) 221801. <https://doi.org/10.1103/PhysRevLett.121.221801>.
- [5] S. P. Behera, D. K. Mishrab, and L. M. Pant, *Sensitivity to sterile neutrino mixing using reactor antineutrinos*, Eur. Phys. J. C 79 (2019) 86. <https://doi.org/10.1140/epjc/s10052-019-6591-0>.
- [6] P. Adamson *et al.* [Daya Bay Collaboration, MINOS + Collaboration], *Improved Constraints on Sterile Neutrino Mixing from Disappearance Searches in the MINOS, MINOS+, Daya Bay, and Bugey-3 Experiments*, Phys. Rev. Lett. 125 (2020) 071801. <https://doi.org/10.1103/PhysRevLett.125.071801>.
- [7] M. G. Aartsen *et al.* [IceCube Collaboration], *Search for an Invisibly Decaying Z' Boson at Belle II in $e^+e^- \rightarrow \mu^+\mu^-(e^\pm\mu^\mp)$ Plus Missing Energy Final States*, Phys. Rev. Lett. 125 (2020) 141801. <https://doi.org/10.1103/PhysRevLett.124.141801>.
- [8] P. Adamson *et al.* (MINOS+ Collaboration), *Search for sterile neutrinos in MINOS and MINOS+ using a two-detector fit*, Phys. Rev. Lett. 122 (2019) 091803. <https://doi.org/10.1103/PhysRevLett.122.091803>.
- [9] A. Aguilar *et al.* (LSND Collaboration), *Evidence for Neutrino Oscillations from the Observation of Electron Anti-neutrinos in a Muon Anti-Neutrino Beam*, Phys. Rev. D 64 (2001) 112007. <https://doi.org/10.1103/PhysRevD.64.112007>.
- [10] M. A. Acero, C. Giunti, and M. Laveder, *Limits on ν_e and $\bar{\nu}_e$ disappearance from Gallium and reactor experiments*, Phys. Rev. D 78 (2008) 073009. <https://doi.org/10.1103/PhysRevD.78.073009>.
- [11] G. Mention *et al.*, *The Reactor Antineutrino Anomaly*, Phys. Rev. D 83 (2011) 073006. <https://doi.org/10.1103/PhysRevD.83.073006>.
- [12] F. P. An *et al.* (Daya Bay Collaboration), *Search for a Light Sterile Neutrino at Daya Bay*, Phys. Rev. Lett. 113 (2014) 141802. <https://doi.org/10.1103/PhysRevLett.113.141802>.
- [13] S. P. Behera, D. K. Mishra, and L. M. Pant, *Active-sterile neutrino mixing constraints using reactor antineutrinos with the ISMRAN setup*, Phys. Rev. D 102 (2020) 013002. <https://doi.org/10.1103/PhysRevD.102.013002>.
- [14] S. K. Kang, Y.-D. Kim, Y.-J. Ko, and K. Siyeon, *Four-neutrino analysis of 1.5km baseline reactor antineutrino oscillations*, Adv. High Energy Phys. 2013 (2013) 138109. <https://doi.org/10.1155/2013/138109>.
- [15] I. Girardi *et. al.*, *Constraining sterile neutrinos using reactor neutrino experiments*, J. High Energ. Phys. 08 (2014) 057. [https://doi.org/10.1007/JHEP08\(2014\)057](https://doi.org/10.1007/JHEP08(2014)057).
- [16] D. C. Rivera-Agudelo and A. Pérez-Lorenzana, *Generating θ_{13} from sterile neutrinos in $\mu - \tau$ symmetric models*, Phys. Rev. D 92 (2015) 073009. <https://doi.org/10.1103/PhysRevD.92.073009>.
- [17] S. Gariazzo *et. al.*, *Updated global 3+1 analysis of short-baseline neutrino oscillations*, J. High Energ. Phys. 2017 (2017) 135. [https://doi.org/10.1007/JHEP06\(2017\)135](https://doi.org/10.1007/JHEP06(2017)135).
- [18] P. Coloma *et. al.*, *Constraining anomalous gluon self-interactions at the LHC: a reappraisal*, J. High Energ. Phys. 07 (2018) 079. [https://doi.org/10.1007/JHEP07\(2018\)093](https://doi.org/10.1007/JHEP07(2018)093).
- [19] J.-H. Liu, S. Zhou, *Another look at the impact of an eV-mass sterile neutrino on the effective neutrino mass of neutrinoless double-beta decays*, Int. J. Mod. Phys. A 33 (2018) 1850014. <https://doi.org/10.1142/S0217751X18500148>.
- [20] S. Gariazzo *et. al.*, *Model-independent $\bar{\nu}_e$ short-baseline oscillations from reactor spectral ratios*, Phys. Lett. B 782 (2018) 13.
- [21] M. Dentler *et. al.*, *Updated global analysis of neutrino oscillations in the presence of eV-scale sterile neutrinos*, J. High Energ. Phys. 08 (2018) 010. [https://doi.org/10.1007/JHEP08\(2018\)010](https://doi.org/10.1007/JHEP08(2018)010).
- [22] S. Gupta *et. al.*, *Effect of a light sterile neutrino at NOvA and DUNE*, Phys. Rev. D 98 (2018) 035042. <https://link.aps.org/doi/10.1103/PhysRevD.98.035042>.
- [23] T. Thakore *et. al.*, *Observation of the decay $\bar{B}_s^0 \rightarrow \chi_{c2} K^+ K^-$ in the ϕ mass region*, J. High Energ. Phys. 08 (2018) 022. [https://doi.org/10.1007/JHEP08\(2018\)191](https://doi.org/10.1007/JHEP08(2018)191).
- [24] S. Dev *et. al.*, *New mixing schemes for (3+1) neutrinos*, Nucl. Phys. B 941 (2019) 401. <https://doi.org/10.1016/j.nuclphysb.2019.02.003>.
- [25] L. S. Miranda and S. Razzaque, *Measurement of the inclusive isolated-photon cross section in pp collisions at $\sqrt{s} = 13$ TeV using 36 fb^{-1} of ATLAS data*, J. High Energ. Phys. 03 (2019) 203. [https://doi.org/10.1007/JHEP10\(2019\)203](https://doi.org/10.1007/JHEP10(2019)203).
- [26] C. Giunti and T. Lasserre, *eV-Scale Sterile Neutrinos*, Annu. Rev. Nucl. Part. Sci. 69 (2019) 163. <https://doi.org/10.1146/annurev-nucl-101918-023755>.
- [27] S. Böser *et. al.*, *Status of Light Sterile Neutrino Searches*, Prog. Part. Nucl. Phys. 111 (2020) 103736. <https://doi.org/10.1016/j.ppnp.2019.103736>.
- [28] C. Giunti *et. al.*, *KATRIN bound on 3+1 active-sterile neutrino mixing and the reactor antineutrino anomaly*, J. High Energ. Phys. 05 (2020) 061. [https://doi.org/10.1007/JHEP05\(2020\)061](https://doi.org/10.1007/JHEP05(2020)061).
- [29] A. Diaz *et. al.*, *Where Are We With Light Sterile Neutrinos?*, Phys. Rep. 884 (2020) 1. <https://doi.org/10.1016/j.physrep.2020.08.005>.
- [30] A. E. Nelson, *Effects of CP violation from neutral heavy fermions on neutrino oscillations, and the LSND/MiniBooNE anomalies*, Phys. Rev. D84 (2011) 053001. <https://doi.org/10.1103/PhysRevD.84.053001>.

- [31] J. Fan and P. Langacker, *Light sterile neutrinos and short baseline neutrino oscillation anomalies*, J. High Energ. Phys. 04 (2012) 083. [https://doi.org/10.1007/JHEP04\(2012\)083](https://doi.org/10.1007/JHEP04(2012)083).
- [32] E. Kuflik, S. D. McDermott, K. M. Zurek, *Neutrino Phenomenology in a 3+1+1 Framework*, Phys. Rev. D86 (2012) 033015. <https://link.aps.org/doi/10.1103/PhysRevD.86.033015>.
- [33] J. Huang and A. E. Nelson, *MeV dark matter in the 3+1+1 model*, Phys. Rev. D88 (2013) 033016. <https://doi.org/10.1103/PhysRevD.88.033016>.
- [34] C. Giunti, M. Laveder, Y.F. Li, H.W. Long, *Pragmatic View of Short-Baseline Neutrino Oscillations*, Phys. Rev. D88 (2013) 073008.
- [35] J. Kopp *et. al.*, *Are There Sterile Neutrinos at the eV Scale?*, Phys. Rev. Lett. 107 (2011) 091801. <https://doi.org/10.1103/PhysRevLett.107.091801>.
- [36] J. Kopp *et. al.*, *Sterile neutrino oscillations: the global picture*, J. High Energ. Phys. 2013 (2013) 50. [https://doi.org/10.1007/JHEP05\(2013\)050](https://doi.org/10.1007/JHEP05(2013)050).
- [37] S. Goswami and W. Rodejohann, *MiniBooNE Results and Neutrino Schemes with 2 sterile Neutrinos: Possible Mass Orderings and Observables related to Neutrino Masses*, J. High Energ. Phys. 0710 (2007) 073. <https://doi.org/10.1088/1126-6708/2007/10/073>.
- [38] M. Sorel *et. al.*, *Combined analysis of short-baseline neutrino experiments in the (3 + 1) and (3 + 2) sterile neutrino oscillation hypotheses*, Phys. Rev. D 70 (2004) 073004. <https://link.aps.org/doi/10.1103/PhysRevD.70.073004>.
- [39] G. Karagiorgi *et. al.*, *Leptonic CP violation studies at MiniBooNE in the (3 + 2) sterile neutrino oscillation hypothesis*, Phys. Rev. D75 (2007) 013011. <https://link.aps.org/doi/10.1103/PhysRevD.75.013011>.
- [40] M. Maltoni and T. Schwetz, *Sterile neutrino oscillations after first MiniBooNE results*, Phys. Rev. D76 (2007) 093005. <https://doi.org/10.1103/PhysRevD.76.093005>.
- [41] G. Karagiorgi *et. al.*, *Viability of $\Delta m^2 \sim 1\text{eV}^2$ sterile neutrino mixing models in light of MiniBooNE electron neutrino and antineutrino data from the Booster and NuMI beamlines*, Phys. Rev. D80 (2009) 073001 [Erratum-ibid.D 81 (2010) 039902]. <https://link.aps.org/doi/10.1103/PhysRevD.80.073001>.
- [42] C. Giunti and M. Laveder, *Pragmatic view of short-baseline neutrino oscillations*, Phys. Rev. D84 (2011) 073008. <https://link.aps.org/doi/10.1103/PhysRevD.88.073008>.
- [43] A. Donini *et. al.*, *Implications of CP-violation in charmed hadrons*, J. High Energ. Phys. (2012) 161. <https://doi.org/10.1088/1742-6596/556/1/012057>.
- [44] M. Archidiacono *et. al.*, *Testing 3+1 and 3+2 neutrino mass models with cosmology and short baseline experiments*, Phys. Rev. D86 (2012) 065028. <https://link.aps.org/doi/10.1103/PhysRevD.86.065028>.
- [45] P. F. de Salas *et. al.*, *2020 Global reassessment of the neutrino oscillation picture*, J. High Energ. Phys. 02 (2021) 071. [https://doi.org/10.1007/JHEP02\(2021\)071](https://doi.org/10.1007/JHEP02(2021)071).
- [46] K. N. Deepthi, S. Goswami, Vishnudath K. N., and T. K. Poddar, $\mu \rightarrow e\gamma$ selecting scalar leptoquark solutions for the $(g - 2)_{e,\mu}$ puzzles, Phys. Rev. D 102 (2020) 015020. <https://link.aps.org/doi/10.1103/PhysRevD.102.075007>.
- [47] I. Esteban *et. al.*, *The fate of hints: updated global analysis of three-flavor neutrino oscillations*, J. High Energ. Phys. 09 (2020) 178. [https://doi.org/10.1007/JHEP09\(2020\)178](https://doi.org/10.1007/JHEP09(2020)178).
- [48] A. C. B. Machado, V. Pleitez, *Quasi-Dirac neutrinos in a model with local $B - L$ symmetry*, J. Phys. G: Nucl. Part. Phys. 40 (2013) 035002. <https://doi.org/10.1088/0954-3899/40/3/035002>.
- [49] V. V. Vien, *3 + 1 active-sterile neutrino mixing in $B - L$ model with $S_3 \times Z_4 \times Z_2$ symmetry for normal neutrino mass ordering*, Eur. Phys. J. C 81 (2021) 416. <https://doi.org/10.1140/epjc/s10052-021-09214-5>.
- [50] J. Barry, W. Rodejohann and H. Zhang, *Light Sterile Neutrinos: Models and Phenomenology*, J. High Energ. Phys. 1107 (2011) 091. [https://doi.org/10.1007/JHEP07\(2011\)091](https://doi.org/10.1007/JHEP07(2011)091).
- [51] J. Barry, W. Rodejohann and H. Zhang, *Sterile neutrinos for warm dark matter and the reactor anomaly in flavor symmetry models*, JCAP 1201 (2012) 052. <https://doi.org/10.1088/1475-7516/2012/01/052>.
- [52] H. Zhang, *Light sterile neutrino in the minimal extended seesaw*, Phys. Lett. B 714 (2012) 262. <https://doi.org/10.1016/j.physletb.2012.06.074>.
- [53] D. Borah, *Non-zero θ_{13} with Unbroken $\mu - \tau$ Symmetry of the Active Neutrino Mass Matrix in the Presence of a Light Sterile Neutrino*, Phys. Rev. D 95 (2017) 035016. <https://doi.org/10.1103/PhysRevD.95.035016>.
- [54] P. Das, A. Mukherjee, *Active and sterile neutrino phenomenology with A_4 based minimal extended seesaw*, M. K. Das, Nucl. Phys. B 941 (2019) 755. <https://doi.org/10.1016/j.nuclphysb.2019.02.024>.
- [55] Neelakshi Sarma, Kalpana Bora, and Debasish Borah, *Compatibility of A_4 Flavour Symmetric Minimal Extended Seesaw with (3 + 1) Neutrino Data*, Eur. Phys. J. C 79 2 (2019) 129. <https://doi.org/10.1140/epjc/s10052-019-6584-z>.
- [56] R. Krishnan, A. Mukherjee and S. Goswami, *Realization of the minimal extended seesaw mechanism and the TM_2 type neutrino mixing*, J. High Energ. Phys. 09 (2020) 050. [https://doi.org/10.1007/JHEP09\(2020\)050](https://doi.org/10.1007/JHEP09(2020)050).
- [57] V. V. Vien, *$B-L$ model with $A_4 \times Z_3 \times Z_4$ symmetry for 3 + 1 active-sterile neutrino mixing*, J. Phys. G: Nucl. Part. Phys. 49 (2022) 085001. <https://doi.org/10.1088/1361-6471/ac6a70>.
- [58] S. Khalil, *Low scale $B - L$ extension of the Standard Model at the LHC*, J. Phys. G 35 (2008) 055001. <https://doi.org/10.1088/0954-3899/35/5/055001>.
- [59] M. Abbas, S. Khalil, *Neutrino masses, mixing and leptogenesis in TeV scale $B - L$ extension of the standard mode*, J. High Energ. Phys. 04 (2008) 056. <https://doi.org/10.1088/1126-6708/2008/04/056>.
- [60] H. Ishimori *et. al.*, *Non-Abelian Discrete Symmetries in Particle Physics*, Prog. Theor. Phys. Suppl. 183 (2010) 1. <https://doi.org/10.1143/PTPS.183.1>.
- [61] P. A. Zyla *et. al.* (Particle Data Group), *Review of Particle Physics*, Prog. Theor. Exp. Phys. 2020, 083C01 (2020). <https://doi.org/10.1093/ptep/ptaa104>.

- [62] Kevin J. Kelly *et. al.*, *Neutrino mass ordering in light of recent data*, Phys. Rev. D 103 (2021) 013004. <https://doi.org/10.1103/PhysRevD.103.013004>.
- [63] C. Jarlskog, *Commutator of the Quark Mass Matrices in the Standard Electroweak Model and a Measure of Maximal CP Nonconservation*, Phys. Rev. Lett. 55 (1985) 1039. <https://doi.org/10.1103/PhysRevLett.55.1039>.
- [64] D.-d. Wu, *Rephasing invariants and CP violation*, Phys. Rev. D 33 (1986) 860. <https://doi.org/10.1103/PhysRevD.33.860>.
- [65] O.W. Greenberg, *Rephasing invariant formulation of CP violation in the Kobayashi-Maskawa framework*, Phys. Rev. D32 (1985) 1841. <https://doi.org/10.1103/PhysRevD.32.1841>.
- [66] M. Mitra, G. Senjanovic, and F. Vissani, *Neutrinoless Double Beta Decay and Heavy Sterile Neutrinos*, Nucl. Phys. B 856 (2012) 26. <https://doi.org/10.48550/arXiv.1108.0004>.
- [67] W. Rodejohann, *Neutrinoless double beta decay and neutrino physics*, J. Phys. G39 (2012) 124008. <https://doi.org/10.1088/0954-3899/39/12/124008> Focus to learn more .
- [68] J. D. Vergados, H. Ejiri and F. Simkovic, *Theory of neutrinoless double beta decay*, Rep. Prog. Phys. 75 (2012) 106301. <https://doi.org/10.1088/0034-4885/75/10/106301>.
- [69] M. Agostini *et al.* (GERDA Collaboration), *Improved limit on neutrinoless double beta decay of ^{76}Ge from GERDA Phase II*, Phys. Rev. Lett. 120 (2018) 132503. <https://doi.org/10.1103/PhysRevLett.120.132503>.
- [70] C. E. Aalseth *et al.* (MAJORANA Collaboration), *Search for Zero-Neutrino Double Beta Decay in ^{76}Ge with the Majorana Demonstrator*, Phys. Rev. Lett. 120 (2018) 132502. <https://doi.org/10.1103/PhysRevLett.120.132502>.
- [71] C. Alduino *et al.* (CUORE collaboration), *First Results from CUORE: A Search for Lepton Number Violation via $0\nu\beta\beta$ Decay of ^{130}Te* , Phys. Rev. Lett. 120 (2018) 132501. <https://doi.org/10.1103/PhysRevLett.120.132501>.
- [72] A. Gando *et al.* (KamLAND-Zen Collaboration), *Search for Majorana Neutrinos Near the Inverted Mass Hierarchy Region with KamLAND-Zen*, Phys. Rev. Lett. 117 (2016) 082503. <https://doi.org/10.1103/PhysRevLett.117.082503>.
- [73] M. Agostini *et al.* (GERDA Collaboration), *Probing Majorana neutrinos with double- β decay*, Science 365 (2019) 1445. <https://doi.org/10.1126/science.aav8613>.
- [74] D. Adams *et al.* (CUORE collaboration), *Improved Limit on Neutrinoless Double-Beta Decay in ^{130}Te with CUORE*, Phys. Rev. Lett. 124 (2020) 122501. <https://doi.org/10.1103/PhysRevLett.124.122501>.
- [75] E. Armengaud *et al.* (CUPID-Mo Collaboration), *New Limit for Neutrinoless Double-Beta Decay of ^{100}Mo from the CUPID-Mo Experiment*, Phys. Rev. Lett. 126 (2021) 181802. <https://doi.org/10.1103/PhysRevLett.126.181802>.
- [76] A. A. Aguilar-Arevalo *et al.* (MiniBooNE Collaboration), *Improved Search for $\bar{\nu}_\mu \rightarrow \bar{\nu}_e$ Oscillations in the MiniBooNE Experiment*, Phys. Rev. Lett. 110 (2013) 161801. <https://doi.org/10.1103/PhysRevLett.110.161801>.
- [77] A. A. Aguilar-Arevalo *et al.* (MiniBooNE Collaboration), *Event Excess in the MiniBooNE Search for $\bar{\nu}_\mu \rightarrow \bar{\nu}_e$ Oscillations*, Phys. Rev. Lett. 105 (2010) 181801. <https://doi.org/10.1103/PhysRevLett.105.181801>.
- [78] A. A. Aguilar-Arevalo *et al.* (MiniBooNE Collaboration), *Significant Excess of ElectronLike Events in the MiniBooNE Short-Baseline Neutrino Experiment*, Phys. Rev. Lett. 121 (2018) 221801. <https://doi.org/10.1103/PhysRevLett.121.221801>.
- [79] S. P. Behera, D. K. Mishrab, and L. M. Pant, *Sensitivity to sterile neutrino mixing using reactor antineutrinos*, Eur. Phys. J. C 79 (2019) 86. <https://doi.org/10.1140/epjc/s10052-019-6591-0>.
- [80] S. P. Behera, D. K. Mishra, and L. M. Pant, *Active-sterile neutrino mixing constraint using reactor antineutrinos with the ISMRAN set-up*, Phys. Rev. D 102 (2020) 013002. <https://doi.org/10.1103/PhysRevD.102.013002>.
- [81] S. Gariazzo, C. Giunti, M. Laveder, and Y. F. Li, *Updated Global 3+1 Analysis of Short-BaseLine Neutrino Oscillations*, J. High Energ. Phys. 06 (2017) 135. [https://doi.org/10.1007/JHEP06\(2017\)135](https://doi.org/10.1007/JHEP06(2017)135).
- [82] K. Hagiwara, R. Liao, A. D. Martin, D. Nomura and T. Teubner, $(g-2)_\mu$ and $\alpha(M_Z^2)$ re-evaluated using new precise data, J. Phys. G 38, 085003 (2011). <https://doi.org/10.1088/0954-3899/38/8/085003>.
- [83] M. Davier, A. Hoecker, B. Malaescu and Z. Zhang, *Reevaluation of the hadronic vacuum polarisation contributions to the Standard Model predictions of the muon $g-2$ and $\alpha(m_Z^2)$ using newest hadronic cross-section data*, Eur. Phys. J. C 77 (2017) 827. <https://doi.org/10.1140/epjc/s10052-017-5161-6>.
- [84] T. Nomura and H. Okada, *One-loop neutrino mass model without any additional symmetries*, Phys. Dark Univ. 26 (2019) 100359. <https://doi.org/10.1016/j.dark.2019.100359>.
- [85] T. Nomura and H. Okada, *Zee-Babu type model with $U(1)_{L_\mu-L_\tau}$ gauge symmetry*, Phys. Rev. D 97 (2018) 095023. <https://doi.org/10.1103/PhysRevD.97.095023>.
- [86] T. Blum *et al.* (RBC and UKQCD Collaborations), *Calculation of the hadronic vacuum polarization contribution to the muon anomalous magnetic moment*, Phys. Rev. Lett. 121 (2018) 022003. <https://link.aps.org/doi/10.1103/PhysRevLett.121.022003>.
- [87] A. Keshavarzi, D. Nomura and T. Teubner, *Muon $g-2$ and $\alpha(M_Z^2)$: a new data-based analysis*, Phys. Rev. D 97 (2018) 114025. <https://doi.org/10.1103/PhysRevD.97.114025>.
- [88] T. Aoyama *et al.*, *The anomalous magnetic moment of the muon in the Standard Model*, Phys. Rept. 887 (2020) 1. <https://doi.org/10.1016/j.physrep.2020.07.006>.
- [89] B. Abi *et al.* (Muon g-2 Collaboration), *Measurement of the Positive Muon Anomalous Magnetic Moment to 0.46 ppm*, Phys. Rev. Lett. 126 (2021) 141801. <https://doi.org/10.1103/PhysRevLett.126.141801>.
- [90] R. A. Diaz, R. Martinez and J. A. Rodriguez, *Phenomenology of lepton flavor violation in 2HDM(3) from $(g-2)(\mu)$ and leptonic decays*, Phys. Rev. D 67 (2003) 075011. <https://doi.org/10.1103/PhysRevD.67.075011>.
- [91] F. Jegerlehner and A. Nyffeler, *The Muon g-2*, Phys. Rept. 477 (2009) 1. <https://doi.org/10.1016/j.physrep.2009.04.003>.
- [92] C. Kelso, H. N. Long, R. Martinez and F. S. Queiroz, *Connection of $g-2_\mu$, electroweak, dark matter, and collider constraints on 331 models*, Phys. Rev. D 90 (2014) 113011. <https://doi.org/10.1103/PhysRevD.90.113011>.
- [93] M. Lindner, M. Platscher and F. S. Queiroz, *A Call for New Physics : The Muon Anomalous Magnetic Moment and*

- Lepton Flavor Violation*, Phys. Rept. 731 (2018) 1. <https://doi.org/10.1016/j.physrep.2017.12.001>.
- [94] K. Kowalska and E. M. Sessolo, *Expectations for the muon $g-2$ in simplified models with dark matter*, J. High Energ. Phys. 2017, 112 (2017). [https://doi.org/10.1007/JHEP09\(2017\)112](https://doi.org/10.1007/JHEP09(2017)112).
- [95] Jun Cao *et al*, *Towards the meV limit of the effective neutrino mass in neutrinoless double-beta decays*, Chinese Phys. C 44 (2020) 031001. <https://doi.org/10.1088/1674-1137/44/3/031001>.
- [96] M. Aker *et al.* (KATRIN collaboration), *Improved Upper Limit on the Neutrino Mass from a Direct Kinematic Method by KATRIN*, Phys. Rev. Lett. 123 (2019) 221802. <https://doi.org/10.1103/PhysRevLett.123.221802>.

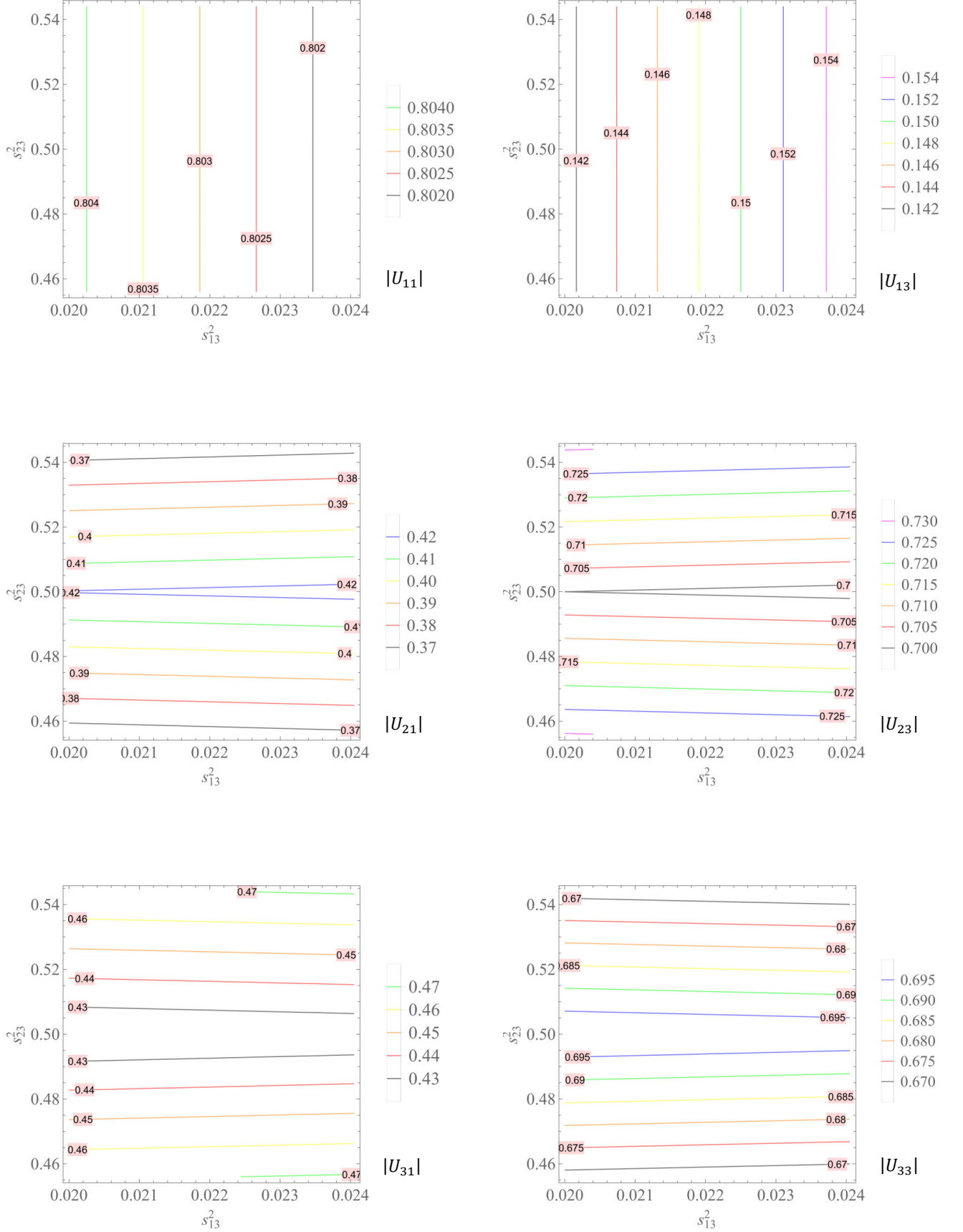


Figure 15: $|U_{ij}|$ ($i = 1, 2, 3; j = 1, 3$) as functions of s_{23}^2 and s_{13}^2 with $s_{23}^2 \in (0.456, 0.544)$ and $s_{13}^2 \in (2.00, 2.405)10^{-2}$ for NH

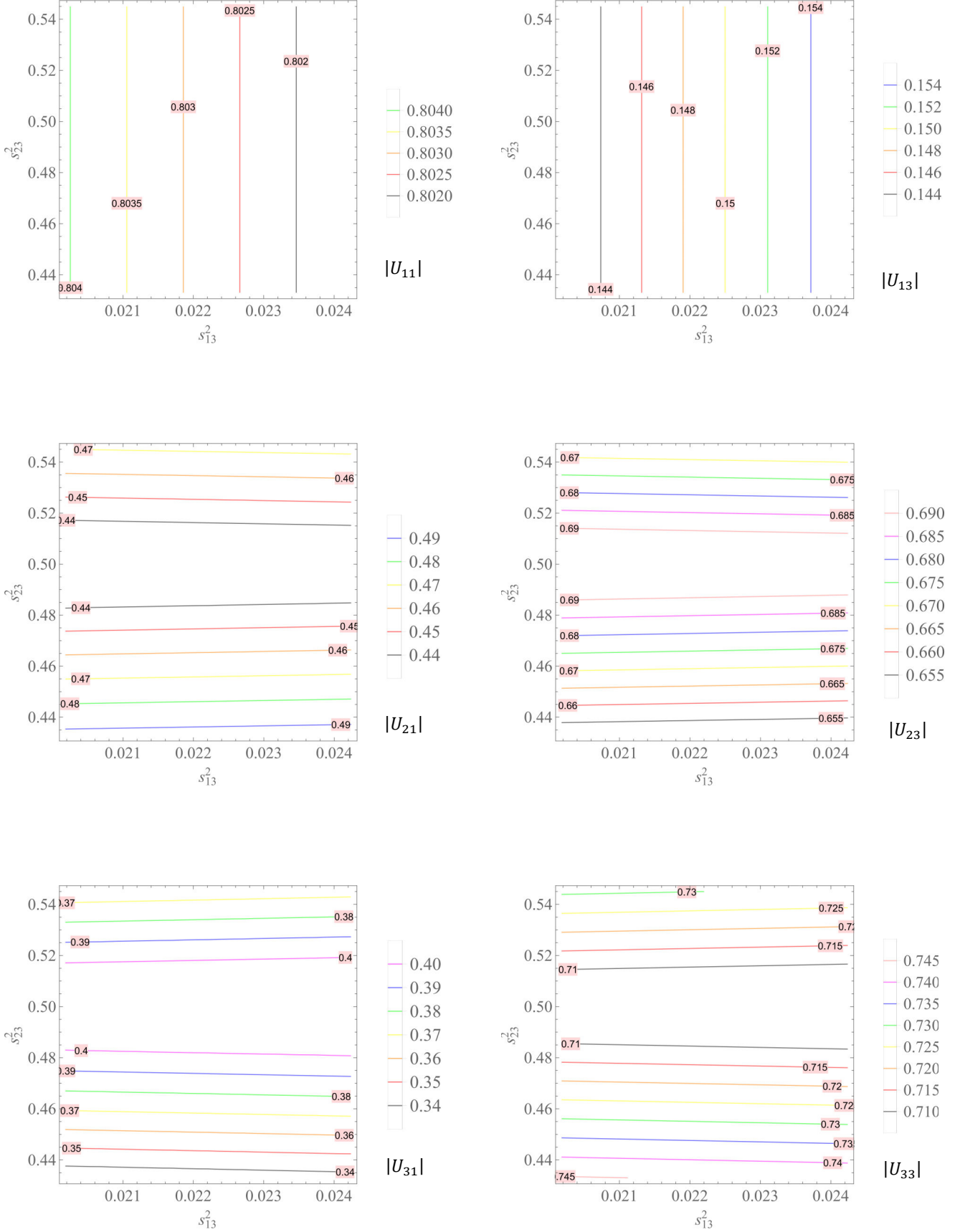


Figure 16: $|U_{ij}|$ ($i = 1, 2, 3; j = 1, 3$) as functions of s_{23}^2 and s_{13}^2 with $s_{23}^2 \in (0.433, 0.545)$ and $s_{13}^2 \in (2.018, 2.242)10^{-2}$ for IH